MAP NO.:	**ASSESSMENT REPORT**	X	**DOCUMENT NO:** 092879
	PROSPECTUS		**MINING DISTRICT:** WATSON LAKE
105 F 7/8/9/10	**CONFIDENTIAL**	X	**TYPE OF WORK:** Geophysics
	OPEN FILE		MAG, VLF EM

REPORT FILED UNDER: Granges Incorporated

DATE PERFORMED: Aug 15-Aug 23, 1990 **DATE FILED:** Oct 9, 1990

LOCATION: **LAT.:** 61°30'N **AREA:** McConnell River

LONG.: 132°30'W **VALUE $:** 48 300

CLAIM NAME & NO.: MATHEW 1-62, 65-146

WORK DONE BY: Aerodat Limited

WORK DONE FOR: Granges Incorporated

DATE TO GOOD STANDING:	

REMARKS: The airborne geophysical survey conducted on the MATHEW claims included magnetic, electromagnetic, and VLF surveys and an interpretation. Conclusions state that several previously unknown structures and trends were outlined.

GEOPHYSICAL REPORT

MATHEW CLAIMS

YB01271-YB01301, YB01456-YB01567, YB01724

SITUATED IN THE McCONNELL RIVER AREA
YUKON TERRITORY

NTS 105/F, Sheets 7, 8, 9, 10
61° 30'N / 132° 30'E

Held under option by

GRANGES INC.
2300-885 WEST GEORGIA STREET
VANCOUVER, BC
V6C 3E8
(604) 687-8699

September 18, 1990

A.J. O'DONNELL
(E.J. Seagel)

This report has been examined by the Geological Evaluation Unit under Section 53 (1) Yukon Quartz Mining Act and is allowed as representation work in the amount of $ 48,308.

for Regional Manager, Exploration and Geological Services for Commissioner of Yukon Territory

TABLE OF CONTENTS

FIGURES

INTRODUCTION

A combined helicopter borne magnetic, electromagnetic and VLF geophysical survey was conducted over the 144 Mathew claims (YB01271-YB01301, YB01456-YB01567, YB01724) from August 15th to August 23rd, 1990.

The claims are held by Granges Inc. of Vancouver, BC, and the program was supervised by Art O'Donnell, Exploration Manager for Granges Inc. A complete schedule of claims is presented in Appendix A.

GEOPHYSICAL SURVEY AND RESULTS

The airborne geophysical survey was comissioned to examine previously indicated soil anomalies, and the program carried out by Aerodat Limited of Mississauga, Ontario.

The Aerodat survey, dated September 13, 1990 and authored by Kevin Killan, geophycisist for Aerodat Limited, accompanies this report as Appendix B.

STATEMENT OF EXPENDITURES

Aerodat invoice 21-9063-0284 is enclosed in Appendix C.

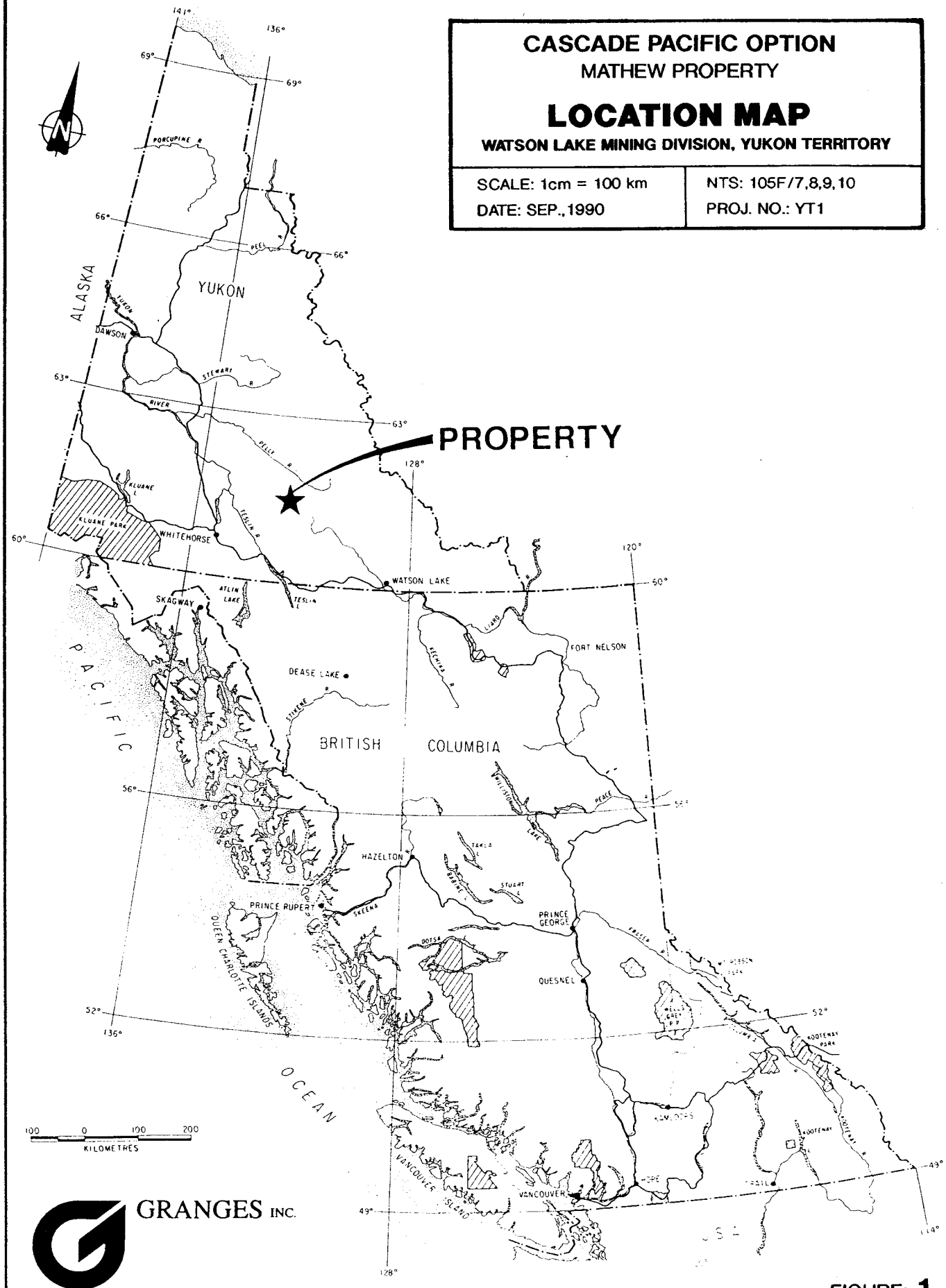
CASCADE PACIFIC OPTION
MATHEW PROPERTY
LOCATION MAP
WATSON LAKE MINING DIVISION, YUKON TERRITORY
SCALE: 1cm = 100 km
DATE: SEP.,1990
NTS: 105F/7,8,9,10
PROJ. NO.: YT1
PROPERTY
ALASKA
YUKON
BRITISH COLUMBIA
PACIFIC OCEAN
DAWSON
WHITEHORSE
WATSON LAKE
SKAGWAY
DEASE LAKE
FORT NELSON
HAZELTON
PRINCE RUPERT
PRINCE GEORGE
QUESNEL
VANCOUVER
VANCOUVER ISLAND
QUEEN CHARLOTTE ISLANDS
KLUANE PARK
KILOMETRES
GRANGES INC.
FIGURE: 1

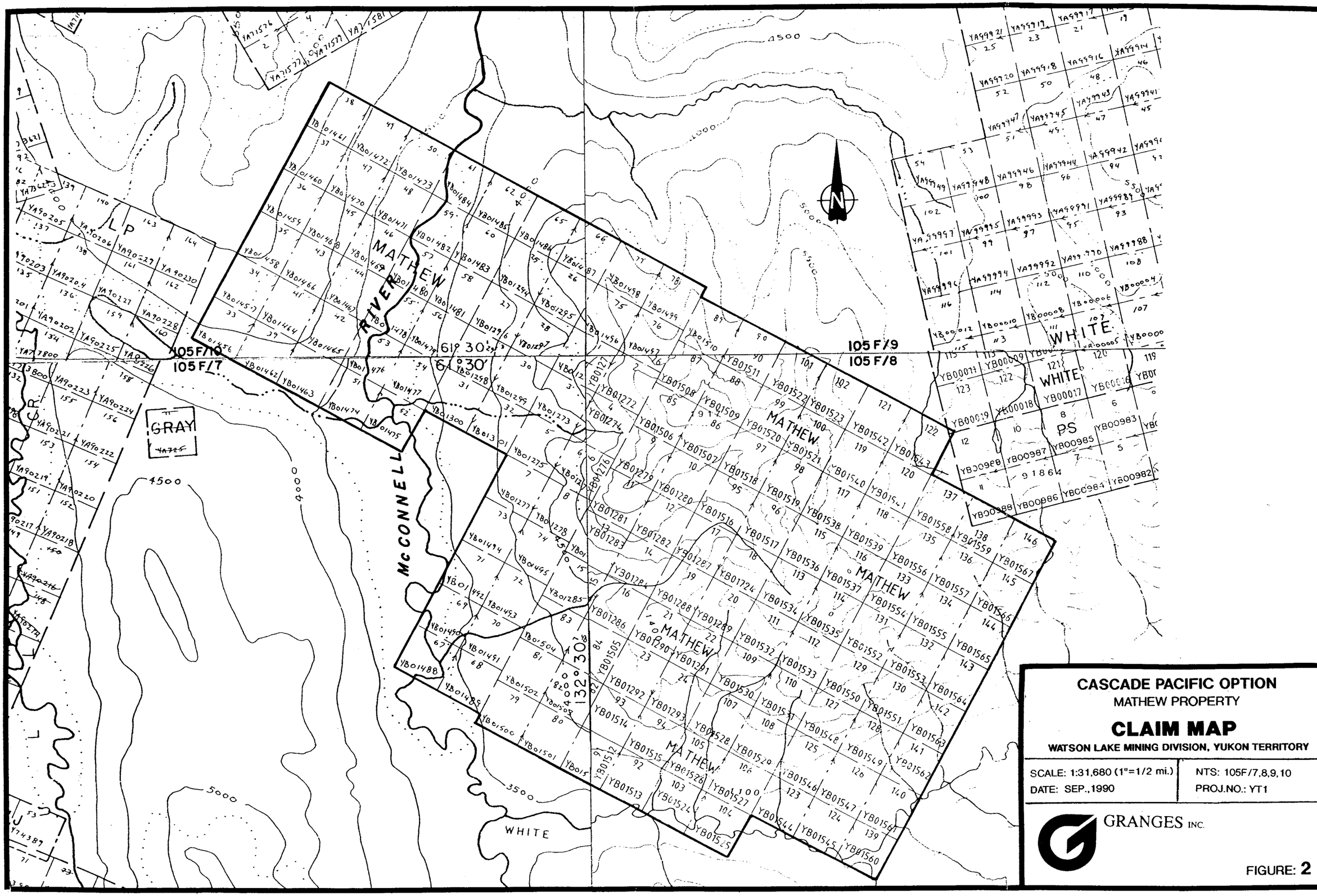

CASCADE PACIFIC OPTION

MATHEW PROPERTY

CLAIM MAP

WATSON LAKE MINING DIVISION, YUKON TERRITORY

SCALE: 1:31,680 (1"=1/2 mi.)	NTS: 105F/7,8,9,10
DATE: SEP.,1990	PROJ.NO.: YT1

GRANGES INC.

FIGURE: **2**

APPENDIX A

SCHEDULE OF CLAIMS

SCHEDULE A

A renewal period of 3 years is requested for each claim.

Claim Number	Claim Name	Due Date	Renewal Period
YB01271	Mathew 1	September 4, 1991	September 4, 1994
YB01272	Mathew 2	September 4, 1991	September 4, 1994
YB01273	Mathew 3	September 4, 1991	September 4, 1994
YB01274	Mathew 4	September 4, 1991	September 4, 1994
YB01275	Mathew 5	September 4, 1991	September 4, 1994
YB01276	Mathew 6	September 4, 1991	September 4, 1994
YB01277	Mathew 7	September 4, 1991	September 4, 1994
YB01278	Mathew 8	September 4, 1991	September 4, 1994
YB01279	Mathew 9	September 4, 1991	September 4, 1994
YB01280	Mathew 10	September 4, 1991	September 4, 1994
YB01281	Mathew 11	September 4, 1991	September 4, 1994
YB01282	Mathew 12	September 4, 1991	September 4, 1994
YB01283	Mathew 13	September 4, 1991	September 4, 1994
YB01284	Mathew 14	September 4, 1991	September 4, 1994
YB01285	Mathew 15	September 4, 1991	September 4, 1994
YB01286	Mathew 16	September 4, 1991	September 4, 1994
YB01287	Mathew 17	September 4, 1991	September 4, 1994
YB01288	Mathew 19	September 4, 1991	September 4, 1994
YB01289	Mathew 20	September 4, 1991	September 4, 1994
YB01290	Mathew 21	September 4, 1991	September 4, 1994
YB01291	Mathew 22	September 4, 1991	September 4, 1994
YB01292	Mathew 23	September 4, 1991	September 4, 1994
YB01293	Mathew 24	September 4, 1991	September 4, 1994
YB01294	Mathew 25	September 4, 1991	September 4, 1994
YB01295	Mathew 26	September 4, 1991	September 4, 1994
YB01296	Mathew 27	September 4, 1991	September 4, 1994
YB01297	Mathew 28	September 4, 1991	September 4, 1994
YB01298	Mathew 29	September 4, 1991	September 4, 1994
YB01299	Mathew 30	September 4, 1991	September 4, 1994
YB01300	Mathew 31	September 4, 1991	September 4, 1994
YB01301	Mathew 32	September 4, 1991	September 4, 1994
YB01456	Mathew 33	September 21, 1990	September 21, 1993
YB01457	Mathew 34	September 21, 1990	September 21, 1993
YB01458	Mathew 35	September 21, 1990	September 21, 1993
YB01459	Mathew 36	September 21, 1990	September 21, 1993
YB01460	Mathew 37	September 21, 1990	September 21, 1993
YB01461	Mathew 38	September 21, 1990	September 21, 1993
YB01462	Mathew 39	September 21, 1990	September 21, 1993
YB01463	Mathew 40	September 21, 1990	September 21, 1993
YB01464	Mathew 41	September 21, 1990	September 21, 1993
YB01465	Mathew 42	September 21, 1990	September 21, 1993
YB01466	Mathew 43	September 21, 1990	September 21, 1993
YB01467	Mathew 44	September 21, 1990	September 21, 1993
YB01468	Mathew 45	September 21, 1990	September 21, 1993
YB01469	Mathew 46	September 21, 1990	September 21, 1993

Claim Number	Claim Name	Due Date	Renewal Period
YB01470	Mathew 47	September 21, 1990	September 21, 1993
YB01471	Mathew 48	September 21, 1990	September 21, 1993
YB01472	Mathew 49	September 21, 1990	September 21, 1993
YB01473	Mathew 50	September 21, 1990	September 21, 1993
YB01474	Mathew 51	September 21, 1990	September 21, 1993
YB01475	Mathew 52	September 21, 1990	September 21, 1993
YB01476	Mathew 53	September 21, 1990	September 21, 1993
YB01477	Mathew 54	September 21, 1990	September 21, 1993
YB01478	Mathew 55	September 21, 1990	September 21, 1993
YB01479	Mathew 56	September 21, 1990	September 21, 1993
YB01480	Mathew 57	September 21, 1990	September 21, 1993
YB01481	Mathew 58	September 21, 1990	September 21, 1993
YB01482	Mathew 59	September 21, 1990	September 21, 1993
YB01483	Mathew 60	September 21, 1990	September 21, 1993
YB01484	Mathew 61	September 21, 1990	September 21, 1993
YB01485	Mathew 62	September 21, 1990	September 21, 1993
YB01486	Mathew 65	September 21, 1990	September 21, 1993
YB01487	Mathew 66	September 21, 1990	September 21, 1993
YB01488	Mathew 67	September 21, 1990	September 21, 1993
YB01489	Mathew 68	September 21, 1990	September 21, 1993
YB01490	Mathew 69	September 21, 1990	September 21, 1993
YB01491	Mathew 70	September 21, 1990	September 21, 1993
YB01492	Mathew 71	September 21, 1990	September 21, 1993
YB01493	Mathew 72	September 21, 1990	September 21, 1993
YB01494	Mathew 73	September 21, 1990	September 21, 1993
YB01495	Mathew 74	September 21, 1990	September 21, 1993
YB01496	Mathew 75	September 21, 1990	September 21, 1993
YB01497	Mathew 76	September 21, 1990	September 21, 1993
YB01498	Mathew 77	September 21, 1990	September 21, 1993
YB01499	Mathew 78	September 21, 1990	September 21, 1993
YB01500	Mathew 79	September 21, 1990	September 21, 1993
YB01501	Mathew 80	September 21, 1990	September 21, 1993
YB01502	Mathew 81	September 21, 1990	September 21, 1993
YB01503	Mathew 82	September 21, 1990	September 21, 1993
YB01504	Mathew 83	September 21, 1990	September 21, 1993
YB01505	Mathew 84	September 21, 1990	September 21, 1993
YB01506	Mathew 85	September 21, 1990	September 21, 1993
YB01507	Mathew 86	September 21, 1990	September 21, 1993
YB01508	Mathew 87	September 21, 1990	September 21, 1993
YB01509	Mathew 88	September 21, 1990	September 21, 1993
YB01510	Mathew 89	September 21, 1990	September 21, 1993
YB01511	Mathew 90	September 21, 1990	September 21, 1993
YB01512	Mathew 91	September 21, 1990	September 21, 1993
YB01513	Mathew 92	September 21, 1990	September 21, 1993
YB01514	Mathew 93	September 21, 1990	September 21, 1993
YB01515	Mathew 94	September 21, 1990	September 21, 1993
YB01516	Mathew 95	September 21, 1990	September 21, 1993
YB01517	Mathew 96	September 21, 1990	September 21, 1993
YB01518	Mathew 97	September 21, 1990	September 21, 1993
YB01519	Mathew 98	September 21, 1990	September 21, 1993
YB01520	Mathew 99	September 21, 1990	September 21, 1993

Claim Number	Claim Name	Due Date	Renewal Period
YB01521	Mathew 100	September 21, 1990	September 21, 1993
YB01522	Mathew 101	September 21, 1990	September 21, 1993
YB01523	Mathew 102	September 21, 1990	September 21, 1993
YB01524	Mathew 103	September 21, 1990	September 21, 1993
YB01525	Mathew 104	September 21, 1990	September 21, 1993
YB01526	Mathew 105	September 21, 1990	September 21, 1993
YB01527	Mathew 106	September 21, 1990	September 21, 1993
YB01528	Mathew 107	September 21, 1990	September 21, 1993
YB01529	Mathew 108	September 21, 1990	September 21, 1993
YB01530	Mathew 109	September 21, 1990	September 21, 1993
YB01531	Mathew 110	September 21, 1990	September 21, 1993
YB01532	Mathew 111	September 21, 1990	September 21, 1993
YB01533	Mathew 112	September 21, 1990	September 21, 1993
YB01534	Mathew 113	September 21, 1990	September 21, 1993
YB01535	Mathew 114	September 21, 1990	September 21, 1993
YB01536	Mathew 115	September 21, 1990	September 21, 1993
YB01537	Mathew 116	September 21, 1990	September 21, 1993
YB01538	Mathew 117	September 21, 1990	September 21, 1993
YB01539	Mathew 118	September 21, 1990	September 21, 1993
YB01540	Mathew 119	September 21, 1990	September 21, 1993
YB01541	Mathew 120	September 21, 1990	September 21, 1993
YB01542	Mathew 121	September 21, 1990	September 21, 1993
YB01543	Mathew 122	September 21, 1990	September 21, 1993
YB01544	Mathew 123	September 21, 1990	September 21, 1993
YB01545	Mathew 124	September 21, 1990	September 21, 1993
YB01546	Mathew 125	September 21, 1990	September 21, 1993
YB01547	Mathew 126	September 21, 1990	September 21, 1993
YB01548	Mathew 127	September 21, 1990	September 21, 1993
YB01549	Mathew 128	September 21, 1990	September 21, 1993
YB01550	Mathew 129	September 21, 1990	September 21, 1993
YB01551	Mathew 130	September 21, 1990	September 21, 1993
YB01552	Mathew 131	September 21, 1990	September 21, 1993
YB01553	Mathew 132	September 21, 1990	September 21, 1993
YB01554	Mathew 133	September 21, 1990	September 21, 1993
YB01555	Mathew 134	September 21, 1990	September 21, 1993
YB01556	Mathew 135	September 21, 1990	September 21, 1993
YB01557	Mathew 136	September 21, 1990	September 21, 1993
YB01558	Mathew 137	September 21, 1990	September 21, 1993
YB01559	Mathew 138	September 21, 1990	September 21, 1993
YB01560	Mathew 139	September 21, 1990	September 21, 1993
YB01561	Mathew 140	September 21, 1990	September 21, 1993
YB01562	Mathew 141	September 21, 1990	September 21, 1993
YB01563	Mathew 142	September 21, 1990	September 21, 1993
YB01564	Mathew 143	September 21, 1990	September 21, 1993
YB01565	Mathew 144	September 21, 1990	September 21, 1993
YB01566	Mathew 145	September 21, 1990	September 21, 1993
YB01567	Mathew 146	September 21, 1990	September 21, 1993
YB01724	Mathew 18	September 21, 1990	September 21, 1993

APPENDIX B

REPORT ON A COMBINED HELICOPTER BORNE MAGNETIC, ELECTROMAGNETIC AND VLF SURVEY MCCONNELL RIVER AREA YUKON TERRITORY

092879

FOR
GRANGES INC.
BY
AERODAT LIMITED
September 13, 1990

J9063

Kevin Killin
Geophysicist

TABLE OF CONTENTS

LIST of MAPS
(Scale 1:10,000)

Basic Maps : (As described under Appendix "B" of Contract)

1. **TOPOGRAPHIC BASE MAP;**
   Showing registration crosses corresponding to NTS coordinates on survey maps, on stable Cronaflex film.

2. **FLIGHT LINES;**
   Photocombination of flight lines, anomalies and fiducials with base map.

3. **AIRBORNE ELECTROMAGNETIC SURVEY INTERPRETATION MAP;**
   showing conductor axes and anomaly peaks along with conductivity thickness values; on a Cronaflex base; Interpretation Report.

4. **TOTAL FIELD MAGNETIC CONTOURS;**
   showing magnetic values contoured at 2 nanoTesla intervals; on a Cronaflex base map.

5. **CALCULATED VERTICAL MAGNETIC GRADIENT CONTOURS;**
   showing vertical gradient values contoured at 0.1 nanoTesla per metre intervals showing flight lines and fiducials; on a Cronaflex base map.

6. **APPARENT RESISTIVITY CONTOURS;**
   calculated from the 4600 Hz coaxial coil pair and contoured in logarithmic intervals (ohm-metres), on the base map.

7. **VLF-EM TOTAL FIELD CONTOURS;**
   of the VLF Total field from the Lualualei, Hawaii transmitter; on a Cronaflex base map.

1. INTRODUCTION

A helicopter borne geophysical survey was carried out for Granges Inc. by Aerodat Ltd. during the period of August 15 - August 23, 1990. Survey equipment included a four frequency electromagnetic system, a cesium vapour high sensitivity magnetometer, a two frequency VLF - EM system and a video tracking camera. The electromagnetic, magnetic, and altimeter data were recorded in both digital and analog forms. The positioning data were encoded on VHS video as well as being marked on the flight path map by the operator. This report and the accompanying maps describe the data collected in this survey.

The survey area is located in the McConnell River area of south central Yukon Territories and is comprised of a single contiguous block. The area was covered in 10 flights with an average line spacing of 100m. Two flight line directions were used, the northwestern portion of the survey block flown in a N30 degrees East orientation, and the southeastern portion in an east-west orientation. The data quality and coverage is considered to be within the contract specifications.

Aerodat Ltd. was contracted to acquire data over and around ground of interest to Granges Inc., and outline any electromagnetic/magnetic anomalies in the survey block. A total of 380 km of data were acquired, compiled, and presented with this report in accordance with specifications laid out by Granges Inc.

2. SURVEY AREA LOCATION

The survey area is located at 61 degrees 30 minutes N, 132 degrees 30 minutes E and lies at the junction of NTS map sheets (105/F 7, 8, 9, 10). It is centred in rough terrain in the Pelly Mountain Range, approximately 50 kilometres south of Ross River. Elevations range from 1000 metres to approximately 1900 metres.

Access to the area can be made by helicopter from Ross River or Whitehorse. A small airstrip is marked by the Ketza River approximately 15 km NE of the survey area and could be used as a base of operations, although the condition of the field is unknown to the writer.

A cut road extends close to the western boundary of the survey area and could also be used for access.

The survey area is depicted in the figure below.

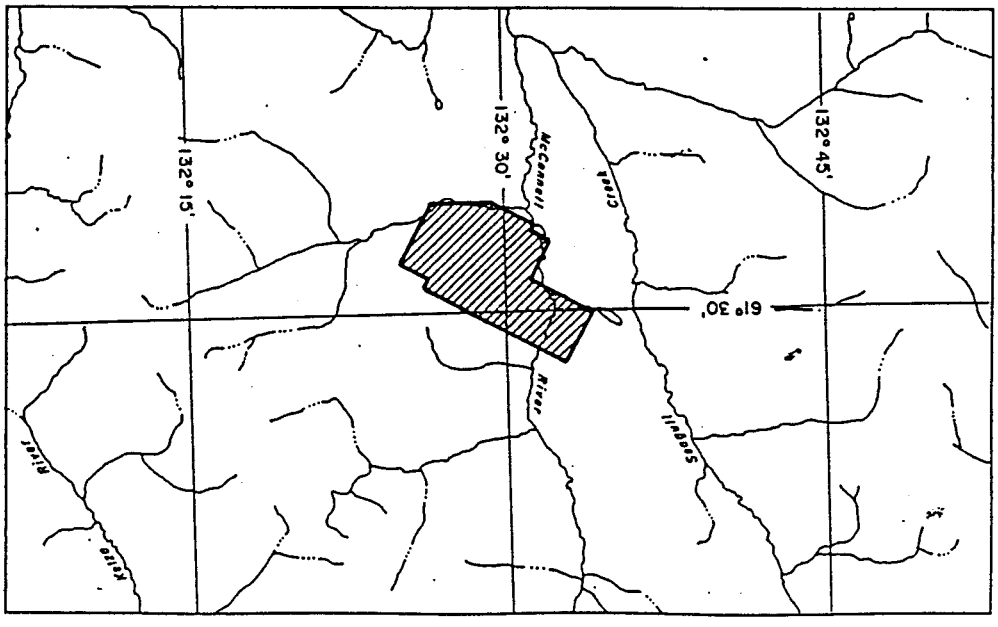

3. AIRCRAFT AND EQUIPMENT

3.1 Aircraft

Due to the rugged terrain, an Aerospatiale SA 315B Lama helicopter, (CG-XYM), piloted by Del Rokosh, owned and operated by Peace Helicopters Limited, was used for the survey. The Aerodat equipment operator and navigator was Mark Barry. Installation of the geophysical and ancillary equipment was carried out by Aerodat. The survey helicopter was flown at a mean terrain clearance of 60 metres, while the EM sensors have a ground clearance of 30 metres.

3.2 Equipment

3.2.1 Electromagnetic System

The electromagnetic system was an Aerodat 4 frequency system. Two vertical coaxial coil pairs are operated at 935 Hz and 4600 Hz and two horizontal coplanar coil pairs at 4175 Hz and 32 kHz. The transmitter-receiver separation was 7 metres. Inphase and quadrature signals were measured simultaneously for the 4 frequencies with a time constant of 0.1 seconds. The electromagnetic bird was towed 30 metres below the helicopter.

3.2.2 VLF-EM System

The VLF-EM System was a Herz Totem 2 A. This instrument measures the total field and quadrature component of the selected frequency. The sensor was

towed in a bird 12 metres below the helicopter. The transmitting station used was NPM, Lualualei, Hawaii broadcasting at 23.4 kHz. This station is maximum coupled with 45 degree striking conductors and provides usable results for strikes +/- 30 degrees.

3.2.3 Magnetometer

The magnetometer employed a Scintrex Model VIW 2321 H8 cesium, optically pumped sensor. The sensitivity of this instrument was 0.1 nanoTeslas at a 0.1 second sampling rate. The sensor was towed in a bird 12 metres below the helicopter.

3.2.4 Magnetic Base Station

An IFG (GEM 8) proton precession magnetometer was operated at the base of operations to record diurnal variations of the earth's magnetic field. The clock of the base station was synchronized with that of the airborne system to facilitate later correlation.

3.2.5 Radar Altimeter

A King KRA 10 radar altimeter was used to record terrain clearance. The output from the instrument is a linear function of altitude for maximum accuracy.

3.2.6 Tracking Camera

A Panasonic video flight path recording system was used to record the flight path on standard VHS format video tapes. The system was operated in continuous mode and the flight number, real time and manual fiducials were registered on the picture frame for cross-reference to the analog and digital data.

3.2.7 Analog Recorder

An RMS dot-Matrix recorder was used to display the data during the survey. In addition to manual and time fiducials, the following data was recorded:

Channel	Input	Scale
CXI1	Low Frequency Inphase Coaxial	25 ppm/cm
CXQ1	Low Frequency Quadrature Coaxial	25
CXI2	High Frequency Inphase Coaxial	25
CXQ2	High Frequency Quadrature Coaxial	25
CPI1	Mid Frequency Inphase Coplanar	100ppm/cm
CPQ1	Mid Frequency Quadrature Coplanar	100
CPI2	High Frequency Inphase Coplanar	200
CPQ2	High Frequency Quadrature Coplanar	200
VLT	VL M Total Field, Line NPM	25 %/cm
VLQ	VL EM Quadrature, Line NPM	25 %/cm
VOT	VLF-EM Total Field,Ortho NSS(NDT)	25 %/cm

VOQ	VLF-EM Quadrature, Ortho NSS(NDT)	25 %/cm
RALT	Radar Altimeter, (150 m. at top of chart)	100ft/cm
MAGF	Magnetometer, fine	25nT/cm
MAGC	Magnetometer, coarse	250nT/cm

3.2.8 Digital Recorder

A DGR 33:16 data system recorded the survey data on magnetic tape. Information recorded was as follows:

Equipment	**Recording Interval**
EM System	0.1 seconds
VLF-EM	0.2 seconds
Magnetometer	0.1 seconds
Altimeter	0.2 seconds
Power Line Monitor	0.2 seconds

4. DATA PRESENTATION

4.1 Base Map

A topographic base map at a scale of 1:10000 was prepared by Aerodat from existing 1:50,000 scale topographic maps. The geophysical data was prepared as overlays on an unscreened Cronaflex base. Registration points corresponding to the Universal Transmercator Grid are shown to ensure accurate registration with base topography.

4.2 Flight Path Map

The flight path was recovered from the VHS video and operator's fiducials that were put on the base map during flight.

The flight lines have time and camera fiducials, flight numbers and line numbers for cross reference with the analog and digital data. Anomaly peaks picked from the 4600 Hz coaxial coils are shown with conductivity thickness ranges and inphase amplitudes.

4.3 Airborne Electromagnetic Interpretation Map

The electromagnetic data was recorded digitally at a sample rate of 10 per second and a time constant of 0.1 seconds. A two stage filtering process was carried out to reject major spheric events and to reduce the system noise.

Local spheric activity can produce sharp, large amplitude events that cannot be removed

by conventional filtering procedures. Smoothing and stacking will reduce their amplitude, but leave broader residual responses that can be confused with geological phenomena. To avoid this possibility, a computer algorithm first searches out and rejects major sferic events.

The signal to noise ratio was further enhanced by the application of a low pass digital filter. It has a zero phase shift which prevents any lag or peak displacement from occurring, and it suppresses only the variations with a wavelength less than about 0.25 seconds. This low effective time constant permits maximum profile shape resolution.

Following the filtering process, a base level correction was made. This correction is a linear function of time that ensures the corrected amplitude of the various inphase and quadrature components is zero when no conductive or permeable source is presented. This filtered and levelled data was used in the electromagnetic interpretation. An interpretation map showing flight lines, conductor axes anomaly peak locations and interpreted structure are presented on a croanflex copy of the base map.

4.4 Total Field Magnetic Contours

The aeromagnetic data have been corrected for diurnal variation by adjustment with the digitally recorded base station data. There has been no correction for regional variation applied. The corrected profile data have been interpolated onto a grid at a 25 m true scale interval using an Akima spline technique. These data were then contoured at a 2

nanoTesla interval and presented on a Cronaflex copy of the base map.

4.5 Calculated Vertical Magnetic Gradient Contours

The vertical magnetic gradient was calculated from the gridded total field magnetic data. These data were then contoured at 0.1 nanoTesla per metre interval and presented on a Cronaflex copy of the base map.

4.6 Apparent Resistivity Contours

The electromagnetic data was processed to yield a map of the apparent resistivity of the ground. The calculations are based on a half space model, i.e. assuming a geological unit with a thickness greater than 200 m. The computer generates a resistivity that would be constant with the bird height and recorded amplitudes for the 4600 Hz coaxial coils. The apparent resistivities calculated for this model were then interpolated onto a grid at a 25 m true scale interval using an Akima spline technique and are presented on a Cronaflex copy of the topographic base map.

4.7 VLF-EM Total Field Contours

The VLF-EM signals from NPM (Lualualei, Hawaii) broadcasting at 23.4 kHz were recorded and presented in contour form on the Cronaflex base map. The orthogonal signals were recorded digitally and may be processed and presented at a later date.

5. INTERPRETATION

5.1 Geology

Geological and previous exploration information was supplied to Aerodat by Granges Inc. as a report entitled "1988 Program of Geological Mapping, Geochemistry and Prospecting on the Mathew Claim Group" (M.J. Burson, January 1989). This report was used as a background source in order to give the writer a better understanding of the area and type of targets sought by Granges. Detail geological information can be found by consulting the aforementioned report.

The region is underlain by a miogeosynclinal sequence of volcanics and carbonates of Devonian/Mississippian age, overlain by phyllites and quartzites. Regional information is believed to be due to a Mesozoic arc-continent collision.

The survey area is underlain by volcaniclastics and sediments and can be divided into two main groups; mafic to intermediate tuffs with minor rhyolite and diorite, and a second group of felsic metavolcanics with rhyolite, chert exhalites, metasediments (quartzite and siltstone).

The mafic to intermediate tuffs have been found to contain siderite/limonite amygdules and frequently contain pyrite.

The felsic tuffs are siliceous containing disseminated pyrite. Pods and beds of pyrite have

also been found. There is abundant sericite and carbonate alteration. Metasediments in the area have been found to contain 95% quartz, up to 5% biotite with disseminated pyrite. Some clasts of pyrite up to 3cm have been found within the quartzite.

There are two noted intrusives in the area, a dark grey magnetic diorite, and a syenite intrusive. The exact location of these is unknown to the author.

Five mineralized zones have been noted, 4 of which are believed to be Kuroko type volcanogenic massive sulfides, and a fifth type composed of Pb, Zn, Ag veins.

5.2 Magnetics

Data obtained from the cesium high sensitivity magnetometer is virtually continuous when reading at .1 second (approx. 3-5 metre) intervals. The sensitivity of 0.1 nT allows for the mapping of very small inflections in the magnetic field.

The magnetic field in the area varies from a low of 58060 nT at the edge of the claims on line 10360, to a peak of greater than 59650 nT in the extreme northeast corner of the survey.

The magnetic map is characterized by a central wide band of gently sloping magnetic data, terminated in the north, south and east by more chaotic, higher amplitude areas.

The map has been divided into six major zones. The first zone is the central, gently sloping, low gradient field. This is terminated to the north by a "step" in the magnetics, which may indicate a lithological change. The step is marked on the interpretation map, and represents a 'geophysical contact', a step ranging from approximately 40 nT in the northwest, to greater than 150 nT in the north central area. This contact may be indicative of the contact between the metasediments to the north and the tuffs to the south, but this can only be validated with a better knowledge of the detail claim geology.

A third zone of magnetics are the elongated magnetic trends running sub-parallel to the inferred contact. These have amplitudes of 50 nT to 100 nT above the surroundings and are found all the way across the contact, virtually always to the south. This may be indicative of some intrusive along the contact, or alternatively a lithology that has been enriched with iron. This horizon is discontinuous, and the contact warped. Faults have been inferred on this basis, along with an examination of the calculated vertical magnetic gradient and small inflections in the magnetic field.

A fourth area of division is located in the north-central part of the map, north of the east-west flight lines and spanning lines 10400-10590. This zone is pod-shaped and there appears to be a 'shelf' of homogeneous magnetics. This is bordered by pods of high magnetic anomalies from 50nT to 200nT above this background.

The high amplitude, discontinuous horizon along the southern border of the claims

constitutes another magnetic horizon. It is believed that this was once a continuous horizon and has been faulted as noted on the interpretation map. This displacement is also noted on the electromagnetic profile map in the area of conductor IX. This horizon may represent mafic volcanics.

The last zone is separated from the area by its high intensity. The peak of 59680 is notably above the regional values and deserves mention.

It should be noted that the Pb, Zn, Ag showing appears to fall on the interpreted geophysical contact, and the gossan zone to the west of the 1988 grid appears to fall between 2 interpreted faults, and on the magnetic anomaly that follows the 'contact'. It should also be noted that the trend of this particular anomaly is NE-SW, which is in contrast to the rest of the oblong anomalies. The NE-SW trend appears to extend to line 10160, which is directly beneath the McConnell river, and along the NW trending fault. The author believes this to be the expression of the McConnell Thrust, or a shear/fracture formed parallel to the thrust.

5.3 Calculated Vertical Magnetic Gradient

The vertical magnetic gradient is calculated from the gridded total field magnetic data. This presentation has the effect of enhancing the high frequency component of the magnetic field. This is essentially equivalent to removing the effects of the regional magnetic field from the data, and enhancing the local, near surface magnetic trends. This gives a fairly

accurate rendition of the local magnetic bodies and trends.

Comparison of the calculated vertical magnetic gradient map with a geological map of the same scale will enable one to see the magnetic 'character' of the geological units. The use of this map can lead to a pseudo-geological map as the zero contour of the calculated vertical magnetic gradient often parallels geologic contacts very closely. The map also enhances trends, and hence it is easier to see their intersection by weak/strong structures.

This map was utilized in parallel with the total field magnetic map to determine the units outlined in the previous section.

5.4 Apparent Resistivity

The apparent resistivity was calculated from the 4600 Hz coaxial coils, assuming a 200m conductive layer, (essentially a half space model). The values vary from less than 10 ohm-metres at the slopes above White Creek, to values in excess of 2000 ohm-metres at the northeastern corner of the survey.

A pronounced low runs from conductor X to IX along the southern edge of the claims. This low runs sub-parallel to the magnetic anomalies noted earlier, and is truncated by the fault trending NE. This is believed to be representative of a conductive lithology parallel to the creek as it lies between 20 and 80m above the creek bed. It may be indicative of talus slopes along the edge of the creek as it seems similar to the low which extends north

along the McConnell River although this trend is not as pronounced.

A resistivity low in area VIII that runs parallel to the mountain slope for a kilometer, is coincident with gossan showings.

A resistivity low is found in the 'nose' of the interpreted contact and at the edge of a fault on line 10450 at 10:25:00. This extends through the contact as a low, although it 'steps' similar to the magnetics.

Line 10410 9:58:00 to 9:58:30 shows a resistivity low along strike with an interpreted fault. This may be an expression of the extension of the fault across the contact.

At the western central edge of the claims, there is a zone co-incident with a magnetic high and approximately 100 ohm-metres lower than the surroundings. The observation that some of the mentioned zones are topographically related, or structurally related may prove useful in explaining the numerous anomalies present after further exploration. It should also be noted that the gossans mentioned earlier seem to be close to resistivity lows and magnetic highs, while the Pb, Zn, Ag veins are related to high resistivity. The expression of the known pyrite beds is not known to the author, although there are anomalous resistivity lows in the vicinity of the 1988 grid.

5.5 VLF-EM Total Field

The signal from NPM, Lualualei, Hawaii, broadcasting at 23.4 kHz was monitored and presented as part of this report. The conductors striking roughly SSW will be the most strongly energized, and as we change the strike further away in either direction the amplitude will drop.

Several conductors are noted, each in a zone of noted electromagnetic conductors. A NE trending zone falls along strike with an interpreted fault, (Zone V) and in the area of the 1988 grid. A NS trending conductor falls south of a resistivity low (and on strike), through zone VI.

A strong conductor trending SE that cuts the north east corner of the survey block goes through a gossan zone, and a resistivity low.

5.6 Electromagnetics

The electromagnetic profiles were first checked by examination of the analog data in conjunction with the presented colour profiles. Record quality is good, although some noise was evident on the analog data. This was easily removed from the data with the application of a spike rejection filter to remove 'spherics', and a smoothing filter to reduce system noise. This procedure has not detracted from data quality or hampered the interpretation of the data.

The electromagnetic anomalies were first picked using a computerized selection program

that was tuned for the ambient and system noise in the area. These selections were plotted with the profile data and selections were added or deleted as deemed necessary. The conductor axes were placed on the map on the basis of similarity of electromagnetic response and correlation with other geophysical data.

The survey area has two distinct conductor groupings. The first group consists of low amplitude conductors with quadrature response, and little inphase, the second group has high responses on all frequencies. The first type is prevalent over the survey area, whereas the high amplitude conductors seem to be mostly confined to the southern border of the survey block. They seem to be coincident with the high amplitude, fractured magnetics in the southern portion of the survey block. The conductors have been grouped into ten groups by the author on the basis of the similarity of strike, response, and correlation with other geophysical data. No attempt has been made to prioritize conductors, and numbers noted on the map are provided for reference between the report and interpretation map.

Conductor group I occurs at the northwestern corner of the survey area. It is composed of two axes striking roughly northwest and correlates with a magnetic anomaly. These low conductance anomalies indicate shallow dip to the south. These conductors are close to the contact noted earlier in the report.

The second conductor group (II) exhibits the same anomaly types as group I and are along strike. They have no magnetic correlation, but run parallel to the magnetic contact.

Group III conductors are near the gossan zone and are located between two interpreted faults. There is a magnetic anomaly extending the length of the conductor and further into the McConnell River valley. The conductor seems to be truncated by the fault running up the valley, although if there has been movement along the fault, group II and III may be of the same origin. It is unknown to the author whether the magnetic anomalies in this area are due to a distinct lithological unit, or are intrusive. Once this has been established it will become simpler to group the conductors more accurately. The conductor dips south.

Group IV is separated from group III by an interpreted fault. They follow the trend of the magnetic anomaly and have less inphase response than group III. The conductor dips the same direction (south). These conductors have shorter strike length (100m-200m) and are bounded to the east and west by faults.

The conductors in Group V cover a large zone. The approximate limits are marked on the interpretation map. These limits seem to encompass the area of intense exploration in 1988. The area is covered by multiple conductor axes. These conductors seem to be very discontinuous in length but are many in number. There is always response noted on the quadrature traces, and there is enough departure between the coplanar and coaxial traces to convince the author that these are bedrock conductors. The profiles become less active in all directions, although the break in the southeast at line 10470 could be questionable. The zone may actually extend to Group VI, which has a similar character. The anomalies indicate a series of flat lying, tabular conductors, and strike generally northwest. There is

no magnetic correlation of these conductors. Conductor group V correlates well with known sulfide occurrences. The anomalies may help to extend known zones when correlated with the know geology.

The seventh group falls in the extreme north west of the survey over an area mapped as graphitic shales on the regional geology map. The conductors have a moderate strike length and higher amplitudes than others in the block. This is consistent with a graphitic shale lithology.

Conductor zone VIII is a group located on the northeastern boundary of the survey area and is in the area of a number of gossans. There are resistivity lows which join the conductors on line 20190 to the zone on 20270 and 20280. These conductors are on the edge of the magnetic anomaly in the northeast corner of the survey. The conductors seem to fall in the zone of low gradient magnetics. These anomalies are primarily quadrature anomalies of low conductance.

Conductors IX and X appear to be part of the same unit. These conductors have the highest conductivity in the area. They are terminated between lines 20220 and 20230, where a fault trends ENE. They correlate well with a highly magnetic unit above the White Creek valley.

5.7 Conclusions & Recommendations

The geophysical survey seems to have outlined some previously unknown structures and trends in the area. The regional deformation and structures inferred by the geophysics leads the writer to believe that more subtle structures will be mapped at a later date. The block is moderately conductive which makes the distinction of bedrock and surficial conductors challenging. A number of conductive zones and trends have been noted. Strike directions and correlation of geophysical data has shown each conductive zone to be of interest for different reasons. Correlation of the known geology and detailed geochemistry will allow the client to prioritize targets, possibly conductors not noted within this report. Ground followup and the correlation of any ground geophysics with this data will help the client to gain a better understanding of the area. Conductors that correlate directly with mapped conductors may warrant ground follow up with detailed ground geophysics, geochemistry, and geological mapping.

Respectfully submitted,

Kevin Killin,
Geophysicist
AERODAT LIMITED
September 13, 1990.

J9063

APPENDIX I

GENERAL INTERPRETIVE CONSIDERATIONS

Electromagnetic

The Aerodat four frequency HEM system uses two different transmitter-receiver coil geometries. The coaxial coils, the optimum configuration for steeply dripping conductors, are typically operated at 900 and 4300 Hz. The coplanar coils, the optimum configuration for flat lying conductors, are typically operated at 4500 and 32000 Hz The near common frequency of 4400 Hz for the two coil configurations is intentional and provides a means for uniquely identifying weakly conductive bedrock sources. The low coaxial frequency is well suited to the detection of good conductors beneath conductive overburden and the high coplanar frequency provides information concerning the more resistive host rocks and overburden covers.

The electromagnetic response measured by the helicopter system is a function of the "electrical" and "geometrical" properties of the conductor. The "electrical" property of a conductor is determined largely by its electrical conductivity, magnetic susceptibility and its size and shape; the "geometrical" property of the response is largely a function of the conductor's shape and orientation with respect to the measuring transmitter and receiver.

Electrical Considerations

For a given conductive body the measure of its conductivity or conductance is closely related to the measured phase shift between the received and transmitted electromagnetic field. A small phase shift indicates a relatively high conductance, a large phase shift lower conductance. A

small phase shift results in a large inphase to quadrature ratio and a large phase shift a low ratio. This relationship is shown quantitatively for a non-magnetic vertical half-plane model on the accompanying phasor diagram. Other physical models will show the same trend but different quantitative relationships.

The phasor diagram for the vertical half-plane model, as presented, is for the coaxial coil configuration with the amplitudes in parts per million (ppm) of the primary field as measured at the response peak over the conductor. To assist the interpretation of the survey results the computer is used to identify the apparent conductance and depth at selected anomalies. The results of this calculation are presented in table form in Appendix IV and the conductance and inphase amplitude are presented in symbolized form on the map presentation.

The conductance and depth values as presented are correct only as far as the model approximates the real geological situation. The actual geological source may be of limited length, have significant dip, may be strongly magnetic, its conductivity and thickness may vary with depth and/or strike and adjacent bodies and overburden may have modified the response. In general the conductance estimate is less affected by these limitations than is the depth estimate, but both should be considered as relative rather than absolute guides to the anomaly's properties.

Conductance in mhos (Siemen) is the reciprocal of resistance in ohms and in the case of narrow slab-like bodies is the product of electrical conductivity and thickness. Most overburden will have an indicated conductance of less than 2 mhos; however, more conductive clays may have

an apparent conductance of say 2 to 4 mhos. Also in the low conductance range will be electrolytic conductors in faults and shears.

The higher ranges of conductance, greater than 4 mhos, indicate that a significant fraction of the electrical conduction is electronic rather than electrolytic in nature. Materials that conduct electronically are limited to certain metallic sulphides and to graphite. High conductance anomalies, roughly 10 mhos or greater, are generally limited to sulphide or graphite bearing rocks.

Sulphide minerals, with the exception of such ore minerals as sphalerite, cinnabar and stibnite, are good conductors; however, sulphides may occur in a disseminated manner that inhibits electrical conduction through the rock mass. In this case the apparent conductance can seriously underrate the quality of the conductor in geological terms. In a similar sense the relatively non-conducting sulphide minerals noted above may be present in significant concentration in association with minor conductive sulphides, and the electromagnetic response only relate to the minor associated mineralization. Indicated conductance is also of little direct significance for the identification of gold mineralization. Although gold is highly conductive, it would not be expected to occur in sufficient quantity to create a recognizable anomaly, but minor accessory sulphide mineralization could provide a useful indirect indication.

In summary, the estimated conductance of a conductor can provide a relatively positive identification of significant sulphide or graphite mineralization; however, a moderate to low

conductance value does not rule out the possibility of significant economic mineralization.

Geometrical Considerations

Geometrical information about the geologic conductor can often be interpreted from the profile shape of the anomaly. The change in shape is primarily related to the change in inductive coupling among the transmitter, the target, and the receiver.

In the case of a thin, steeply dipping, sheet-like conductor, the coaxial coil pair will yield a near symmetric peak over the conductor. On the other hand, the coplanar coil pair will pass through a null couple relationship and yield a minimum over the conductor, flanked by positive side lobes. As the dip of the conductor decreases from vertical, the coaxial anomaly shape changes only slightly, but in the case of the coplanar coil pair the side lobe on the down dip side strengthens relative to that on the up dip side.

As the thickness of the conductor increases, induced current flow across the thickness of the conductor becomes relatively significant and complete null coupling with the coplanar coils is no longer possible. As a result, the apparent minimum of the coplanar response over the conductor diminishes with increasing thickness, and in the limiting case of a fully 3 dimensional body or a horizontal layer or half-space, the minimum disappears completely.

A horizontal conducting layer such as overburden will produce a response in the coaxial and coplanar coils that is a function of altitude (and conductivity if not uniform). The profile shape

will be similar in both coil configurations with an amplitude ratio (coplanar/coaxial) of about 4:1*.

In the case of a spherical conductor, the induced currents are confined to the volume of the sphere, but not restricted to any arbitrary plane as in the case of a sheet-like form. The response of the coplanar coil pair directly over the sphere may be up to 8* times greater than that of the coaxial pair.

In summary, a steeply dipping, sheet-like conductor will display a decrease in the coplanar response coincident with the peak of the coaxial response. The relative strength of this coplanar null is related inversely to the thickness of the conductor; a pronounced null indicates a relatively thin conductor. The dip of such a conductor can be inferred from the relative amplitudes of the side-lobes.

Massive conductors that could be approximated by a conducting sphere will display a simple single peak profile form on both coaxial and coplanar coils, with a ratio between the coplanar to coaxial response amplitudes as high as 8*.

Overburden anomalies often produce broad poorly defined anomaly profiles. In most cases, the response of the coplanar coils closely follows that of the coaxial coils with a relative amplitude ration of 4*.

Occasionally, if the edge of an overburden zone is sharply defined with some significant depth extent, an edge effect will occur in the coaxial coils. In the case of a horizontal conductive ring or ribbon, the coaxial response will consist of two peaks, one over each edge; whereas the coplanar coil will yield a single peak.

* It should be noted at this point that Aerodat's definition of the measured ppm unit is related to the primary field sensed in the receiving coil without normalization to the maximum coupled (coaxial configuration). If such normalization were applied to the Aerodat units, the amplitude of the coplanar coil pair would be halved.

Magnetics

The Total Field Magnetic Map shows contours of the total magnetic field, uncorrected for regional variation. Whether an EM anomaly with a magnetic correlation is more likely to be caused by a sulphide deposit than one without depends on the type of mineralization. An apparent coincidence between an EM and a magnetic anomaly may be caused by a conductor which is also magnetic, or by a conductor which lies in close proximity to a magnetic body. The majority of conductors which are also magnetic are sulphides containing pyrrhotite and/or magnetite. Conductive and magnetic bodies in close association can be, and often are, graphite and magnetite. It is often very difficult to distinguish between these cases. If the conductor is also magnetic, it will usually produce an EM anomaly whose general pattern resembles that of the magnetics. Depending on the magnetic permeability of the conducting body, the amplitude of the inphase EM anomaly will be weakened, and if the conductivity is also weak, the inphase

EM anomaly may even be reversed in sign.

Apparent Resistivity/Conductivity Maps

Overburden and different types of bedrock may be modelled as a large area horizontal conductor of fixed thickness. A phasor diagram may be constructed, in the same fashion as for the vertical sheet, to convert the measured HEM in-phase and quadrature response to a depth and conductivity value for a horizontal layer. Traditionally if the thickness is large, an infinite half-space, the associated conductivity value is referred to as "apparent conductivity". We have generalized the use of the word "apparent" to include any model where the thickness of the layer is a fixed as opposed to a variable parameter. The units of apparent resisitivity are ohm-m and those of apparent conductivity are the inverse mhos/m or siemen/m. If the chosen model layer thickness is close to the true thickness of the conductor then the apparent conductivity will closely conform to the true value; however, if the thickness is inappropriate the apparent value may be considerably different from the true value.

The benefit of the apparent conductivity mapping is that it provides a simple robust method of converting the HEM in-phase and quadrature response to apparent change in ground conductivity.

A phasor diagram for several apparent resistivity models is presented. The general forms for the various thicknesses is very similar and also closely resembles the diagram for the vertical sheet. The diagrams also show the curves for apparent depth. As with the conductivity value the depth value is meaningful if the model thickness closely resembles the true conductive layer thickness.

If the HEM response from a thin conducting layer is applied to a thick layer model the apparent conductivity and depth will be less than the true conductivity and depth.

VLF Electromagnetics

The VLF-EM method employs the radiation from powerful military radio transmitters as the primary signals. The magnetic field associated with the primary field is elliptically polarized in the vicinity of electrical conductors. The Herz Totem uses three coils in the X, Y, Z configuration to measure the total field and vertical quadrature component of the polarization ellipse.

The relatively high frequency of VLF (15-25) kHz provides high response factors for bodies of low conductance. Relatively "disconnected" sulphide ores have been found to produce measurable VLF signals. For the same reason, poor conductors such as sheared contacts, breccia zones, narrow faults, alteration zones and porous flow tops normally produce VLF anomalies. The method can therefore be used effectively for geological mapping. The only relative disadvantage of the method lies in its sensitivity to conductive overburden. In conductive ground the depth of exploration is severely limited.

The effect of strike direction is important in the sense of the relation of the conductor axis relative to the energizing electromagnetic field. A conductor aligned along a great circle radius drawn from a transmitting station will be in a maximum coupled orientation and thereby produce a stronger response than a similar conductor at a different strike angle. Theoretically, it would

be possible for a conductor, oriented tangentially to the transmitter to produce no signal. The most obvious effect of the strike angle consideration is that conductors favourably oriented with respect to the transmitter location and also near perpendicular to the flight direction are most clearly rendered and usually dominate the map presentation.

The total field response is an indicator of the existence and position of a conductivity anomaly. The response will be a maximum over the conductor, without any special filtering, and strongly favour the upper edge of the conductor even in the case of a relatively shallow dip.

The vertical quadrature component over steeply dipping sheet-like conductor will be a cross-over type response with the cross-over closely associated with the upper edge of the conductor. The quandrature response is a cross-over type due to the fact that it is the vertical rather than total field component that is measured. The response shape is due largely to geometrical rather than conductivity considerations and the distance between the maximum and minimum on either side of the cross-over is related to target depth. For a given target geometry, the larger this distance the greater the depth.

The amplitude of the quadrature response, as opposed to shape is function of target conductance and depth as well as the conductivity of the overburden and host rock. As the primary field travels down to the conductor through conductive material it is both attenuated and phase shifted in a negative sense. The secondary field produced by this altered field at the target also has an associated phase shift. This phase shift is positive and is larger for relatively poor conductors.

This secondary field is attenuated and phase shifted in a negative sense during return travel to the surface. The net effect of these 3 phase shifts determine the phase of the secondary field sensed at the receiver.

A relatively poor conductor in resistive ground will yield a net positive phase shift. A relatively good conductor in more conductive ground will yield a net negative phase shift. A combination is possible whereby the net phase shift is zero and the response is purely in-phase with no quadrature component.

A net positive phase shift combined with the geometrical cross-over shape will lead to a positive quadrature response on the side of aircraft approach and a negative on the side of departure. A net negative phase shift would produce the reverse. A further sign reversal occurs with a 180 degree change in instrument orientation as occurs on reciprocal line headings. During digital processing of the quadrature data for map presentation this is corrected for by normalizing the sign to one of the flight line headings.

APPENDIX II

ANOMALY LIST

McConnell River Area

FLIGHT	LINE	ANOMALY	CATEGORY	AMPLITUDE (PPM) INPHASE	QUAD.	CONDUCTOR CTP MHOS	DEPTH MTRS	BIRD HEIGHT MTRS
1	10010	B	1	17.9	26.3	0.7	0	42
1	10010	C	1	12.4	20.4	0.5	0	42
1	10010	D	1	11.1	17.4	0.5	0	48
1	10010	E	1	6.3	16.6	0.2	0	49
1	10010	F	1	16.8	24.5	0.7	0	43
1	10010	G	0	1.9	15.0	0.0	0	49
1	10020	A	0	1.0	2.0	0.1	0	125
1	10020	B	1	12.7	16.4	0.8	0	45
1	10020	C	1	6.9	17.3	0.2	0	44
1	10020	D	2	11.6	12.2	1.0	0	60
1	10020	E	1	9.7	11.8	0.7	0	64
1	10020	F	0	3.4	17.4	0.0	0	58
1	10020	G	1	13.0	28.8	0.3	0	53
1	10020	H	1	21.6	42.2	0.5	0	49
1	10030	A	1	38.4	63.7	0.9	0	35
1	10030	B	1	51.2	94.3	0.8	0	35
1	10030	C	1	10.1	29.8	0.2	0	37
1	10030	D	1	9.2	22.4	0.2	0	49
1	10030	E	1	7.4	10.9	0.5	0	61
1	10030	F	2	15.7	17.0	1.1	0	41
1	10030	G	2	19.3	21.0	1.2	0	39
1	10030	H	1	16.7	20.8	0.9	0	40
1	10040	A	0	1.5	6.2	0.0	0	54
1	10040	B	0	1.8	9.7	0.0	0	38
1	10040	C	0	2.3	9.5	0.0	0	43
1	10040	D	1	8.3	16.2	0.3	0	44
1	10040	E	1	6.5	14.1	0.2	0	54
1	10040	F	1	18.9	24.6	0.9	0	45
1	10040	G	2	20.8	25.4	1.0	0	43
1	10040	H	0	4.5	14.3	0.1	0	43
1	10040	J	0	4.4	31.3	0.0	0	42
1	10040	K	0	4.7	25.3	0.0	0	41
1	10040	M	0	10.1	34.2	0.1	0	45
1	10050	A	2	67.0	113.2	1.0	0	32
1	10050	B	1	12.2	41.3	0.2	0	36
1	10050	C	1	11.3	24.4	0.3	0	39
1	10050	D	1	20.6	34.4	0.7	0	41
1	10050	E	1	13.7	36.5	0.3	0	37
1	10050	F	0	2.2	6.6	0.1	0	50
1	10050	G	1	12.8	18.8	0.6	0	47

Estimated depth may be unreliable because the stronger part of the conductor may be deeper or to one side of the flight line, or because of a shallow dip or overburden effects.

McConnell River Area

FLIGHT	LINE	ANOMALY	CATEGORY	AMPLITUDE (PPM) INPHASE	QUAD.	CONDUCTOR CTP MHOS	DEPTH MTRS	BIRD HEIGHT MTRS
1	10050	H	1	13.3	19.2	0.7	0	48
1	10050	J	0	3.8	11.6	0.1	0	52
1	10060	A	1	2.3	4.3	0.2	0	68
1	10060	B	0	1.3	5.2	0.0	0	49
1	10060	C	0	1.8	5.1	0.0	2	46
1	10060	D	0	4.7	12.6	0.1	0	40
1	10060	E	1	6.0	10.0	0.4	0	51
1	10060	F	2	18.0	20.9	1.0	0	44
1	10060	G	1	17.2	21.1	0.9	0	40
1	10060	H	0	2.7	7.9	0.1	1	40
1	10060	J	0	1.9	9.1	0.0	0	45
1	10060	K	1	11.5	38.5	0.2	0	39
1	10060	M	1	14.1	40.5	0.2	0	41
1	10060	N	1	9.1	26.4	0.2	0	48
1	10070	B	1	47.0	103.2	0.6	0	34
1	10070	C	1	11.5	28.1	0.3	0	41
1	10070	D	1	15.5	28.2	0.5	0	41
1	10070	E	1	15.4	37.1	0.3	0	39
1	10070	F	1	12.8	16.1	0.8	0	45
1	10070	G	0	2.5	13.8	0.0	0	40
1	10080	A	0	4.5	14.0	0.1	0	38
1	10080	B	1	7.7	12.6	0.4	0	47
1	10080	C	1	8.2	12.0	0.5	0	51
1	10080	D	0	2.2	27.7	0.0	0	39
1	10080	E	0	7.8	56.5	0.0	0	29
1	10090	C	2	13.8	11.5	1.5	0	63
1	10090	D	1	22.1	34.1	0.8	0	47
1	10090	E	1	7.8	19.9	0.2	0	44
1	10090	F	0	3.9	15.4	0.0	0	43
1	10100	A	0	1.3	3.9	0.0	0	79
1	10100	B	1	3.5	3.7	0.6	1	67
1	10100	C	1	3.1	3.9	0.4	0	65
1	10100	D	0	2.3	6.3	0.1	0	46
1	10100	E	0	2.2	4.7	0.1	2	52
1	10100	F	0	4.6	13.7	0.1	0	48
1	10100	G	0	2.4	13.0	0.0	0	45
1	10100	H	1	7.3	17.7	0.2	0	34
1	10100	J	1	7.7	17.8	0.2	0	35
1	10100	K	1	4.4	9.4	0.2	0	47
1	10100	M	0	4.7	12.7	0.1	0	46

Estimated depth may be unreliable because the stronger part of the conductor may be deeper or to one side of the flight line, or because of a shallow dip or overburden effects.

McConnell River Area

FLIGHT	LINE	ANOMALY	CATEGORY	AMPLITUDE (PPM) INPHASE	AMPLITUDE (PPM) QUAD.	CONDUCTOR CTP MHOS	CONDUCTOR DEPTH MTRS	BIRD HEIGHT MTRS
1	10100	N	0	7.0	33.3	0.1	0	36
1	10100	O	0	9.2	34.0	0.1	0	39
1	10110	A	3	24.1	14.5	2.8	0	53
1	10110	B	3	25.9	18.0	2.4	0	56
1	10110	C	1	26.2	47.1	0.7	0	33
1	10110	D	1	11.0	35.1	0.2	0	35
1	10110	E	0	3.9	12.4	0.1	0	45
1	10110	F	0	3.8	13.9	0.1	0	39
1	10110	G	0	1.1	6.8	0.0	0	43
1	10120	B	0	3.8	9.5	0.1	0	65
1	10120	C	1	4.7	10.7	0.2	0	57
1	10120	D	1	7.0	14.2	0.3	0	46
1	10120	E	1	7.8	11.7	0.5	2	40
1	10120	F	1	9.3	11.9	0.7	1	42
1	10120	G	1	9.8	15.2	0.5	0	39
1	10120	H	1	5.9	9.2	0.4	0	50
1	10120	J	1	6.8	11.2	0.4	0	50
1	10120	K	1	5.7	13.8	0.2	0	45
1	10120	M	1	12.5	28.6	0.3	0	43
1	10120	N	1	15.1	28.1	0.5	0	47
1	10120	O	2	30.2	27.4	1.8	0	47
1	10130	B	1	10.2	12.8	0.7	0	54
1	10130	C	1	7.2	13.8	0.3	0	38
1	10130	D	1	7.1	14.5	0.3	0	36
1	10130	E	1	4.1	7.8	0.2	5	41
1	10130	F	1	3.8	7.5	0.2	4	42
1	10140	C	1	12.2	19.3	0.6	0	45
1	10140	D	1	9.2	14.4	0.5	0	42
1	10140	E	2	13.0	14.4	1.0	0	42
1	10140	F	2	10.6	9.7	1.2	1	48
1	10140	G	1	10.9	13.2	0.8	0	43
1	10140	H	1	14.6	22.3	0.6	0	45
1	10140	J	1	10.1	20.3	0.4	0	37
1	10140	K	1	15.3	23.3	0.7	0	45
1	10140	M	1	26.3	36.4	0.9	0	38
1	10140	N	3	40.5	30.3	2.5	0	42
1	10150	A	4	34.8	13.5	5.7	0	70
1	10150	B	1	35.7	78.7	0.6	0	30
1	10150	C	1	12.6	14.5	0.9	0	41
1	10150	D	1	15.5	19.0	0.9	0	48

Estimated depth may be unreliable because the stronger part of the conductor may be deeper or to one side of the flight line, or because of a shallow dip or overburden effects.

McConnell River Area

FLIGHT	LINE	ANOMALY	CATEGORY	AMPLITUDE (PPM) INPHASE	QUAD.	CONDUCTOR CTP MHOS	DEPTH MTRS	BIRD HEIGHT MTRS
1	10150	E	2	10.5	7.9	1.5	3	49
1	10150	F	1	8.6	9.6	0.8	3	45
1	10150	G	1	10.4	16.5	0.5	4	33
1	10150	H	1	12.2	19.9	0.5	0	41
1	10150	J	1	11.0	23.4	0.3	0	42
1	10160	B	1	14.8	28.7	0.5	0	45
1	10160	C	1	16.8	34.2	0.4	0	38
1	10160	D	1	15.3	47.0	0.2	0	38
1	10160	E	1	17.0	39.0	0.4	0	41
1	10160	F	2	17.5	17.2	1.3	0	49
1	10160	G	1	20.7	31.0	0.8	0	42
1	10160	H	3	30.9	20.8	2.6	0	46
1	10160	J	4	49.1	26.9	4.0	0	50
1	10170	A	4	35.2	17.5	4.1	0	56
1	10170	B	4	48.9	23.4	4.8	0	59
1	10170	C	4	45.0	22.7	4.4	0	55
1	10180	B	2	28.2	30.7	1.3	0	44
1	10180	C	2	19.2	14.9	1.8	0	52
1	10180	D	3	59.2	35.3	3.8	0	47
1	10180	E	3	72.6	49.5	3.4	0	41
1	10180	F	3	71.8	51.8	3.2	0	39
1	10190	A	4	85.5	42.4	5.4	0	39
1	10190	B	4	96.0	53.0	4.9	0	39
1	10190	C	3	85.5	55.1	3.9	0	42
1	10200	A	3	6.8	3.0	2.8	35	34
1	10200	B	3	6.5	2.5	3.3	17	55
1	10200	C	1	7.9	13.5	0.4	0	42
1	10200	D	2	7.7	6.2	1.2	16	41
1	10200	E	2	14.6	15.3	1.1	0	53
1	10210	A	4	38.7	19.2	4.2	0	48
1	10210	B	3	47.8	26.8	3.9	0	46
1	10210	C	1	18.5	33.0	0.6	0	46
1	10210	D	0	10.9	1.6	14.9	2	62
1	10210	E	2	8.1	5.1	1.8	11	50
1	10210	F	3	7.2	3.9	2.1	21	44
1	10220	B	2	6.2	3.5	1.9	22	46
1	10220	C	1	8.7	9.4	0.8	0	65
1	10220	D	2	19.0	17.8	1.4	0	55

Estimated depth may be unreliable because the stronger part of the conductor may be deeper or to one side of the flight line, or because of a shallow dip or overburden effects.

McConnell River Area

FLIGHT	LINE	ANOMALY	CATEGORY	AMPLITUDE (PPM) INPHASE	AMPLITUDE (PPM) QUAD.	CONDUCTOR CTP MHOS	CONDUCTOR DEPTH MTRS	BIRD HEIGHT MTRS
1	10220	E	2	38.5	39.2	1.6	0	42
1	10230	A	3	26.3	19.4	2.2	0	50
1	10240	A	2	14.3	14.9	1.1	0	45
1	10240	B	2	16.0	17.7	1.1	0	41
1	10240	C	1	13.7	41.8	0.2	0	36
1	10240	D	1	14.9	21.5	0.7	0	42
1	10240	E	1	26.8	45.5	0.7	0	41
1	10250	A	2	31.8	37.0	1.3	0	49
1	10250	B	2	34.1	45.7	1.1	0	42
1	10250	C	2	10.2	7.2	1.7	1	53
1	10250	D	3	10.4	6.1	2.2	6	51
1	10250	E	3	10.3	5.3	2.6	12	46
1	10250	F	3	6.9	3.9	2.0	31	35
1	10250	G	3	7.7	3.3	3.0	24	43
1	10260	A	4	10.3	3.0	5.7	13	50
1	10260	B	0	12.4	1.4	22.2	11	51
1	10260	C	0	11.2	1.4	18.7	15	49
1	10260	D	4	8.1	2.1	6.2	12	57
1	10260	E	3	25.4	20.0	2.0	0	52
1	10260	F	2	27.4	22.4	1.9	0	50
1	10260	G	2	20.6	19.5	1.4	0	43
1	10260	H	1	19.9	30.3	0.7	0	48
1	10270	A	1	14.9	18.3	0.9	0	41
1	10270	B	2	14.6	16.1	1.0	0	47
1	10270	C	1	7.6	8.5	0.8	14	36
1	10270	D	1	8.2	8.4	0.9	13	38
1	10270	E	2	14.8	14.9	1.2	1	40
1	10270	F	3	23.7	15.6	2.5	0	45
1	10270	G	4	9.2	2.5	6.1	15	51
1	10280	A	4	10.9	3.4	5.3	23	38
1	10280	B	3	6.6	3.2	2.4	23	46
1	10280	C	1	7.1	14.6	0.3	0	42
1	10280	D	1	11.0	21.5	0.4	0	33
1	10280	E	2	7.6	6.7	1.1	4	52
1	10280	F	0	4.9	26.4	0.0	0	35
1	10280	G	2	36.2	37.4	1.6	0	45
1	10280	H	3	43.6	34.8	2.4	0	43
2	10290	B	2	30.5	32.1	1.4	0	49

Estimated depth may be unreliable because the stronger part of the conductor may be deeper or to one side of the flight line, or because of a shallow dip or overburden effects.

McConnell River Area

FLIGHT	LINE	ANOMALY	CATEGORY	AMPLITUDE (PPM) INPHASE	QUAD.	CONDUCTOR CTP MHOS	DEPTH MTRS	BIRD HEIGHT MTRS
2	10290	C	1	5.9	13.9	0.2	0	43
2	10290	D	0	6.5	19.3	0.1	0	43
2	10290	E	0	2.6	7.9	0.1	4	36
3	10300	C	1	7.5	11.7	0.5	13	29
3	10300	D	1	7.1	10.0	0.5	0	55
3	10310	A	2	21.0	19.6	1.5	0	49
3	10310	B	2	15.2	11.1	1.8	0	54
3	10310	C	1	8.6	12.9	0.5	0	48
3	10310	D	1	7.0	16.3	0.2	0	54
3	10310	E	1	6.1	14.2	0.2	0	59
3	10310	F	0	4.3	12.9	0.1	0	49
3	10310	G	0	2.8	10.8	0.0	0	51
3	10310	H	0	0.3	10.1	0.0	0	38
3	10320	A	1	2.7	3.9	0.3	17	46
3	10320	B	1	2.7	4.8	0.2	8	48
3	10320	C	0	0.8	7.4	0.0	0	41
3	10320	D	0	0.7	8.6	0.0	0	36
3	10320	E	0	0.4	8.7	0.0	0	38
3	10320	F	0	7.0	25.0	0.1	0	37
3	10320	G	0	3.6	15.4	0.0	0	50
3	10330	A	1	10.6	13.0	0.8	0	60
3	10330	B	1	8.1	11.8	0.5	0	63
3	10330	C	1	7.0	10.7	0.5	0	57
3	10330	D	1	3.6	5.5	0.3	0	64
3	10330	E	1	3.8	5.9	0.3	0	65
3	10330	F	1	5.5	12.9	0.2	0	57
3	10330	G	1	7.8	10.9	0.5	16	28
3	10330	H	1	7.7	12.3	0.4	0	50
3	10330	J	1	7.0	12.8	0.3	11	28
3	10330	K	1	5.6	10.6	0.3	16	26
3	10330	M	1	5.1	7.7	0.4	11	38
3	10340	B	0	2.0	6.1	0.0	10	34
3	10340	C	0	1.5	4.3	0.0	14	37
3	10340	D	0	2.0	9.7	0.0	0	39
3	10340	E	0	1.8	8.7	0.0	0	43
3	10340	F	1	8.5	21.6	0.2	0	43
3	10340	G	0	3.9	9.8	0.1	0	69
3	10350	A	1	10.7	11.6	0.9	0	55
3	10350	B	1	10.2	13.1	0.7	0	54

Estimated depth may be unreliable because the stronger part of the conductor may be deeper or to one side of the flight line, or because of a shallow dip or overburden effects.

McConnell River Area

FLIGHT	LINE	ANOMALY	CATEGORY	AMPLITUDE (PPM) INPHASE	QUAD.	CONDUCTOR CTP MHOS	DEPTH MTRS	BIRD HEIGHT MTRS
3	10350	C	1	4.5	5.8	0.5	5	51
3	10350	D	1	8.0	11.6	0.5	16	27
3	10350	E	1	6.1	15.3	0.2	0	64
3	10350	F	1	5.2	12.6	0.2	7	30
3	10350	G	1	4.7	11.1	0.2	1	37
3	10360	A	1	3.7	2.9	0.9	8	67
3	10360	B	0	1.8	6.9	0.0	1	38
3	10360	C	1	3.1	6.5	0.2	13	35
3	10360	D	0	1.4	5.6	0.0	0	49
3	10360	E	0	-2.3	13.0	0.0	0	41
3	10360	F	1	8.6	17.7	0.3	0	38
3	10360	G	1	7.6	17.5	0.2	0	39
3	10360	H	1	3.4	6.5	0.2	0	50
3	10360	J	1	5.6	10.3	0.3	0	49
3	10360	K	0	2.7	10.2	0.0	7	27
3	10370	A	1	5.3	8.2	0.4	0	51
3	10370	B	1	5.4	5.3	0.8	9	51
3	10370	C	1	6.4	8.8	0.5	0	68
3	10370	D	1	8.2	10.8	0.6	10	35
3	10370	E	1	8.5	8.6	0.9	12	38
3	10370	F	1	7.3	20.0	0.2	0	32
3	10370	G	1	6.1	15.0	0.2	0	40
3	10380	B	0	-3.1	5.3	0.0	0	37
3	10380	C	0	2.3	6.5	0.1	0	79
3	10380	D	0	4.0	11.8	0.1	0	39
3	10380	E	0	4.3	11.0	0.1	0	45
3	10380	F	1	4.4	9.0	0.2	4	39
3	10380	G	0	3.0	9.1	0.1	0	42
3	10380	H	0	2.0	11.8	0.0	0	35
3	10380	J	1	3.7	6.7	0.2	5	44
3	10380	K	0	0.2	5.8	0.0	0	48
3	10380	M	0	2.2	8.0	0.0	0	71
4	10390	A	0	3.8	11.4	0.1	0	55
4	10390	B	1	5.6	11.7	0.2	11	28
4	10390	C	1	2.9	6.0	0.2	0	55
4	10390	D	1	6.3	9.3	0.5	11	35
4	10390	E	1	6.9	8.5	0.6	0	52
4	10390	F	1	5.4	5.3	0.8	1	59
4	10390	G	0	3.3	8.7	0.1	0	63
4	10390	H	0	1.3	6.3	0.0	0	57
4	10390	J	1	3.4	7.5	0.2	0	45

Estimated depth may be unreliable because the stronger part of the conductor may be deeper or to one side of the flight line, or because of a shallow dip or overburden effects.

McConnell River Area

FLIGHT	LINE	ANOMALY	CATEGORY	AMPLITUDE (PPM) INPHASE	QUAD.	CONDUCTOR CTP MHOS	DEPTH MTRS	BIRD HEIGHT MTRS
4	10390	K	0	3.3	1.4	2.2	45	45
4	10390	M	0	0.0	4.9	0.0	0	63
4	10400	A	1	3.8	4.8	0.5	26	34
4	10400	B	0	1.4	0.9	0.8	58	54
4	10400	C	0	0.2	10.4	0.0	0	55
4	10400	D	0	3.4	11.1	0.1	0	42
4	10400	E	0	2.0	6.6	0.0	0	51
4	10400	F	0	2.7	8.5	0.1	0	54
4	10400	G	0	2.4	9.7	0.0	0	47
4	10400	H	1	4.1	7.0	0.3	8	41
4	10400	J	0	1.3	6.0	0.0	0	51
4	10410	A	1	5.7	12.1	0.2	9	29
4	10410	B	3	6.2	3.3	2.1	29	40
4	10410	C	0	2.9	9.3	0.1	0	67
4	10410	D	1	8.1	15.8	0.3	6	30
4	10410	E	1	10.6	21.9	0.3	0	40
4	10410	F	1	5.4	8.9	0.4	0	47
4	10410	G	1	3.0	5.6	0.2	14	38
4	10410	H	0	1.4	1.3	0.4	48	51
4	10410	J	0	1.1	7.5	0.0	0	35
4	10410	K	0	2.0	7.6	0.0	0	43
4	10410	M	0	2.6	6.1	0.1	0	56
4	10410	N	0	2.4	8.6	0.0	0	48
4	10420	B	0	3.8	12.7	0.1	0	46
4	10420	C	0	4.9	12.7	0.1	0	62
4	10420	D	1	6.4	16.9	0.2	0	38
4	10420	E	1	7.6	18.0	0.2	0	41
4	10420	F	1	6.7	8.7	0.6	13	35
4	10430	A	2	5.9	4.4	1.2	31	34
4	10430	B	0	3.7	11.2	0.1	0	54
4	10430	C	0	4.2	12.9	0.1	0	59
4	10430	D	1	10.2	19.5	0.4	0	44
4	10430	E	1	7.9	20.4	0.2	0	35
4	10430	F	1	5.5	9.6	0.3	9	35
4	10440	A	0	3.7	1.1	3.9	43	47
4	10440	B	0	2.4	9.3	0.0	0	45
4	10440	C	0	3.4	12.1	0.1	0	52
4	10440	D	1	7.0	15.8	0.2	0	42
4	10450	A	1	5.1	4.5	0.9	17	47

Estimated depth may be unreliable because the stronger part of the conductor may be deeper or to one side of the flight line, or because of a shallow dip or overburden effects.

McConnell River Area

FLIGHT	LINE	ANOMALY	CATEGORY	AMPLITUDE (PPM) INPHASE	QUAD.	CONDUCTOR CTP MHOS	DEPTH MTRS	BIRD HEIGHT MTRS
4	10450	B	1	7.5	15.6	0.3	0	45
4	10450	C	1	8.6	18.1	0.3	2	31
4	10450	D	0	-0.8	6.9	0.0	0	69
4	10460	B	0	2.0	1.6	0.7	30	62
4	10460	C	0	3.6	0.3	23.6	27	69
4	10460	D	1	3.2	3.8	0.5	10	56
4	10460	E	0	1.9	8.3	0.0	8	27
4	10460	F	2	5.0	3.3	1.4	44	27
4	10460	G	0	4.1	10.5	0.1	8	30
4	10460	H	0	4.6	12.4	0.1	0	41
4	10460	J	0	4.1	1.4	3.3	19	66
4	10470	C	1	3.7	5.5	0.3	26	30
4	10480	A	0	3.3	1.8	1.5	7	79
4	10480	B	1	2.8	3.4	0.4	26	42
4	10480	C	0	4.1	1.3	3.7	42	44
4	10490	B	1	4.1	4.5	0.6	13	50
4	10490	C	0	4.2	20.3	0.0	0	36
4	10490	D	0	4.3	16.7	0.1	0	39
4	10490	E	0	2.2	9.0	0.0	0	37
4	10510	B	1	4.4	4.0	0.8	21	46
4	10510	C	0	3.3	8.2	0.1	0	42
4	10510	D	1	6.9	13.6	0.3	1	37
4	10510	E	1	6.5	13.5	0.3	0	43
4	10510	F	1	5.5	9.9	0.3	6	37
4	10510	G	1	6.0	10.8	0.3	2	40
4	10510	H	0	-0.1	9.8	0.0	0	40
5	10520	A	1	4.7	5.8	0.5	0	59
5	10520	B	1	5.9	9.1	0.4	0	46
5	10520	C	1	6.2	8.6	0.5	15	33
5	10520	D	0	0.7	4.6	0.0	0	55
5	10520	E	0	2.2	1.3	1.2	28	69
5	10520	F	0	4.7	1.5	3.9	0	95
5	10520	G	1	2.1	2.3	0.4	0	81
7	10530	A	1	3.2	6.4	0.2	0	53
7	10530	B	1	5.7	8.6	0.4	0	58
7	10530	C	0	2.1	5.2	0.1	0	52
7	10530	D	0	1.6	5.1	0.0	6	41
7	10530	E	1	2.4	2.9	0.4	0	78

Estimated depth may be unreliable because the stronger part of the conductor may be deeper or to one side of the flight line, or because of a shallow dip or overburden effects.

McConnell River Area

FLIGHT	LINE	ANOMALY	CATEGORY	AMPLITUDE (PPM) INPHASE	QUAD.	CONDUCTOR CTP MHOS	DEPTH MTRS	BIRD HEIGHT MTRS
7	10550	B	0	1.6	16.3	0.0	0	41
7	10550	C	0	0.5	1.6	0.0	10	60
7	10550	D	0	-1.1	2.8	0.0	0	67
7	10560	A	0	1.3	9.8	0.0	0	62
7	10560	B	0	4.0	11.4	0.1	0	63
7	10570	A	1	3.6	4.5	0.4	0	82
7	10570	B	1	5.0	4.8	0.8	5	57
7	10570	C	1	4.8	4.2	0.9	5	60
7	10580	A	1	3.3	4.9	0.3	16	42
7	10590	D	3	7.8	3.2	3.2	12	55
7	10590	E	0	3.7	1.8	1.9	0	130
7	10590	F	0	2.9	1.6	1.4	0	123
7	10600	A	0	3.3	1.9	1.4	2	83
7	10600	B	1	4.2	4.1	0.7	0	70
7	10610	A	0	1.1	3.8	0.0	0	60
7	10620	A	1	3.7	3.2	0.8	21	51
7	10630	A	1	2.6	2.1	0.8	34	50
7	10640	A	1	2.7	5.5	0.2	0	54
6	20010	A	0	5.1	20.5	0.1	0	54
6	20020	D	0	7.0	43.2	0.0	0	34
6	20020	J	1	15.5	44.2	0.3	0	43
6	20020	K	0	9.1	31.9	0.1	0	46
6	20030	A	1	6.2	10.7	0.4	0	50
6	20030	B	1	13.2	38.6	0.2	0	50
6	20030	C	1	13.5	38.2	0.2	0	42
6	20030	F	0	7.1	39.3	0.0	0	39
6	20030	G	1	8.1	22.5	0.2	0	37
6	20030	H	1	4.8	11.9	0.2	0	74
6	20040	A	1	6.8	18.9	0.2	0	55
6	20040	B	1	16.1	45.6	0.3	0	36
6	20040	C	1	6.9	10.3	0.5	0	83

Estimated depth may be unreliable because the stronger part of the conductor may be deeper or to one side of the flight line, or because of a shallow dip or overburden effects.

McConnell River Area

FLIGHT	LINE	ANOMALY	CATEGORY	AMPLITUDE (PPM) INPHASE	QUAD.	CONDUCTOR CTP MHOS	DEPTH MTRS	BIRD HEIGHT MTRS
6	20050	A	1	12.1	24.6	0.4	0	49
6	20050	B	1	20.0	36.3	0.6	0	43
6	20050	C	2	17.1	15.6	1.4	1	40
6	20050	D	2	6.1	4.5	1.3	0	72
6	20050	E	1	6.8	13.8	0.3	0	50
6	20050	F	1	4.5	10.1	0.2	0	56
6	20050	G	0	9.0	35.7	0.1	0	40
6	20060	A	2	16.4	15.3	1.3	0	55
6	20070	A	2	21.9	22.6	1.3	0	42
6	20070	B	1	14.1	20.7	0.7	0	42
6	20070	C	1	16.4	29.5	0.5	0	37
6	20070	D	2	17.9	19.7	1.1	0	52
6	20070	E	3	19.4	13.6	2.1	1	42
6	20070	F	3	35.2	25.0	2.6	0	43
6	20070	G	3	34.9	25.7	2.4	0	41
6	20070	H	3	31.8	20.1	2.9	0	48
6	20070	J	3	14.9	6.8	3.5	0	55
6	20080	B	3	17.0	11.8	2.0	2	43
6	20080	C	4	55.4	27.4	4.8	0	37
6	20080	D	4	85.6	50.3	4.4	0	36
6	20080	E	3	87.4	58.1	3.7	0	37
6	20080	F	2	25.7	33.6	1.0	0	41
6	20080	G	1	20.1	31.2	0.7	0	43
6	20090	A	1	9.5	11.7	0.7	2	42
6	20090	B	1	9.4	12.4	0.7	2	41
6	20090	C	2	24.7	27.3	1.2	0	37
6	20090	D	3	31.3	21.4	2.6	2	35
6	20090	G	3	78.9	54.9	3.4	0	38
6	20090	K	4	78.3	39.5	5.2	0	48
6	20090	M	2	29.4	24.6	1.9	2	33
6	20090	N	1	5.7	8.0	0.5	0	54
6	20090	O	2	6.6	5.5	1.1	3	57
6	20100	B	2	20.2	17.1	1.7	1	39
6	20100	C	4	36.8	15.1	5.4	0	51
6	20100	D	4	120.3	63.6	5.5	0	40
6	20100	G	3	67.3	61.1	2.3	0	36
6	20110	A	1	10.1	14.3	0.6	0	59
6	20110	B	1	11.4	15.3	0.7	0	60

Estimated depth may be unreliable because the stronger part of the conductor may be deeper or to one side of the flight line, or because of a shallow dip or overburden effects.

McConnell River Area

FLIGHT	LINE	ANOMALY	CATEGORY	AMPLITUDE (PPM) INPHASE	QUAD.	CONDUCTOR CTP MHOS	DEPTH MTRS	BIRD HEIGHT MTRS
6	20110	C	2	62.2	65.3	1.9	0	34
6	20110	D	3	58.2	53.0	2.2	0	41
6	20110	E	4	84.0	39.6	5.8	0	54
6	20110	F	2	15.0	10.8	1.9	0	64
6	20110	J	0	3.2	8.2	0.1	0	49
6	20110	K	1	4.0	7.4	0.2	0	49
6	20110	M	0	2.8	7.9	0.1	0	55
6	20120	A	0	1.7	5.2	0.0	0	47
6	20120	B	0	1.0	6.6	0.0	0	41
6	20120	C	3	40.4	30.9	2.4	0	38
6	20120	D	3	34.5	27.8	2.2	0	46
6	20120	E	3	24.7	12.2	3.7	0	51
6	20120	F	2	18.1	17.4	1.3	0	44
6	20120	G	2	14.1	14.7	1.1	0	54
6	20130	A	0	1.6	5.5	0.0	0	58
6	20130	B	0	1.2	7.6	0.0	0	56
6	20130	C	1	6.3	13.0	0.3	0	42
6	20130	D	1	7.6	15.9	0.3	0	52
6	20130	E	2	14.3	15.4	1.0	0	49
6	20130	F	3	27.4	19.6	2.3	0	50
6	20130	G	3	25.3	15.7	2.7	0	62
6	20130	H	3	39.0	27.7	2.6	0	37
6	20140	A	1	10.3	21.4	0.3	4	27
6	20140	B	3	25.8	16.3	2.7	0	58
6	20140	C	3	31.5	26.2	2.0	0	44
6	20140	D	2	20.2	18.4	1.5	0	48
6	20140	E	2	11.2	9.7	1.3	0	54
6	20150	A	2	4.3	2.3	1.8	2	77
6	20150	B	0	5.0	1.8	3.3	5	74
6	20150	C	0	3.4	9.0	0.1	0	41
6	20150	D	2	30.0	25.3	1.9	0	55
6	20150	E	3	38.1	21.0	3.7	0	60
6	20150	F	4	12.0	3.3	6.5	0	70
6	20150	G	0	4.6	17.9	0.1	0	40
6	20160	A	4	11.0	3.6	5.0	13	48
6	20160	B	4	13.1	4.1	5.6	2	55
6	20160	C	3	22.5	10.4	3.9	0	67
6	20160	E	4	30.8	14.3	4.3	0	64
6	20160	F	2	27.4	22.4	1.9	0	62
6	20160	G	2	8.6	6.3	1.5	19	38

Estimated depth may be unreliable because the stronger part of the conductor may be deeper or to one side of the flight line, or because of a shallow dip or overburden effects.

McConnell River Area

FLIGHT	LINE	ANOMALY	CATEGORY	AMPLITUDE (PPM) INPHASE	QUAD.	CONDUCTOR CTP MHOS	DEPTH MTRS	BIRD HEIGHT MTRS
6	20160	H	2	7.3	5.4	1.4	38	22
6	20160	J	0	4.5	11.9	0.1	0	37
7	20170	A	0	10.9	39.3	0.1	0	48
7	20170	B	0	14.9	61.3	0.1	0	39
7	20170	C	1	13.7	47.6	0.2	0	42
7	20170	D	1	9.7	11.4	0.8	0	45
7	20170	M	1	16.5	34.0	0.4	0	46
7	20170	N	1	7.5	12.5	0.4	3	37
7	20170	O	1	5.3	6.2	0.6	11	45
7	20170	P	2	5.6	4.0	1.3	0	79
7	20170	Q	2	17.3	15.6	1.4	0	58
7	20180	A	1	8.8	15.2	0.4	0	53
7	20180	B	2	10.1	8.4	1.3	0	51
7	20180	C	2	6.5	4.0	1.7	0	66
7	20180	D	1	17.8	32.0	0.6	0	43
7	20180	J	3	42.1	35.4	2.2	0	47
7	20180	K	2	25.7	23.6	1.6	0	58
7	20180	M	1	12.1	31.9	0.3	0	48
7	20190	A	1	21.1	85.9	0.2	0	30
7	20190	B	2	16.0	13.4	1.5	0	46
7	20190	C	3	26.8	18.7	2.4	0	48
7	20190	D	3	32.2	23.9	2.3	0	56
7	20190	G	2	53.3	61.3	1.6	0	33
7	20190	H	2	10.2	9.9	1.1	0	51
7	20190	J	3	6.3	3.3	2.1	21	48
7	20190	K	2	5.1	3.1	1.6	24	48
7	20190	M	2	5.6	3.3	1.7	33	37
7	20190	N	0	3.2	7.6	0.1	0	52
7	20190	O	0	5.5	16.7	0.1	1	30
7	20190	P	1	6.0	11.2	0.3	0	58
7	20190	Q	1	4.2	9.2	0.2	0	44
7	20190	R	1	6.3	7.2	0.7	0	94
8	20200	A	0	0.6	2.2	0.0	0	97
8	20200	B	0	1.6	6.6	0.0	0	61
8	20200	C	1	6.6	12.8	0.3	4	35
8	20200	D	0	1.5	10.9	0.0	0	52
8	20200	E	0	3.2	14.9	0.0	0	60
8	20200	F	3	40.3	31.2	2.4	0	52
8	20200	G	2	22.7	25.1	1.2	0	45
8	20200	H	1	15.6	61.4	0.2	0	40
8	20210	A	0	24.7	124.0	0.1	0	28

Estimated depth may be unreliable because the stronger part of the conductor may be deeper or to one side of the flight line, or because of a shallow dip or overburden effects.

McConnell River Area

FLIGHT	LINE	ANOMALY	CATEGORY	AMPLITUDE (PPM) INPHASE	QUAD.	CONDUCTOR CTP MHOS	DEPTH MTRS	BIRD HEIGHT MTRS
8	20210	B	1	25.8	119.4	0.2	0	28
8	20210	C	1	25.4	110.2	0.2	0	29
8	20210	D	1	22.3	90.3	0.2	0	32
8	20210	E	3	62.4	51.4	2.6	0	47
8	20210	F	0	6.2	20.2	0.1	0	45
8	20210	G	0	6.7	20.1	0.1	0	47
8	20210	H	1	8.7	18.1	0.3	0	44
8	20210	J	1	3.9	7.4	0.2	0	83
8	20210	K	1	5.0	5.0	0.7	8	53
8	20210	M	1	4.8	4.9	0.7	0	61
8	20210	N	1	4.6	5.9	0.5	18	38
8	20210	O	0	2.7	7.1	0.1	7	37
8	20210	P	0	2.8	8.4	0.1	0	57
8	20220	A	1	4.1	9.2	0.2	0	70
8	20220	B	1	6.5	7.0	0.7	9	45
8	20220	C	1	5.8	5.2	0.9	6	55
8	20220	D	0	3.7	12.5	0.1	0	55
8	20220	E	0	3.1	7.7	0.1	0	63
8	20220	F	2	5.7	4.9	1.0	15	47
8	20220	G	0	4.1	0.5	14.4	43	48
8	20220	H	0	0.5	11.9	0.0	0	57
8	20220	J	1	17.9	29.8	0.6	0	35
8	20220	K	3	69.9	67.3	2.2	0	39
8	20220	M	1	33.0	49.7	0.9	0	35
8	20230	A	1	28.1	129.8	0.2	0	33
8	20230	B	1	26.6	99.4	0.2	0	35
8	20230	C	1	10.2	11.3	0.9	0	63
8	20230	D	2	20.9	24.2	1.1	0	53
8	20230	E	0	1.4	6.7	0.0	7	30
8	20230	F	0	0.9	10.5	0.0	0	54
8	20230	G	0	0.7	9.9	0.0	0	45
8	20230	H	0	-0.6	4.7	0.0	0	78
8	20230	J	0	2.3	12.2	0.0	0	45
8	20230	K	1	4.5	8.6	0.2	0	49
8	20230	M	0	2.0	12.2	0.0	0	59
8	20240	A	0	2.3	9.1	0.0	0	60
8	20240	B	0	2.3	12.7	0.0	0	35
8	20240	C	0	2.1	8.0	0.0	0	52
8	20240	D	0	0.5	0.3	0.5	94	68
8	20240	E	2	31.0	43.2	1.0	0	34
8	20240	F	2	32.9	43.0	1.1	0	38
8	20250	A	1	11.6	28.1	0.3	0	39

Estimated depth may be unreliable because the stronger part of the conductor may be deeper or to one side of the flight line, or because of a shallow dip or overburden effects.

McConnell River Area

FLIGHT	LINE	ANOMALY	CATEGORY	AMPLITUDE (PPM) INPHASE	AMPLITUDE (PPM) QUAD.	CONDUCTOR CTP MHOS	CONDUCTOR DEPTH MTRS	BIRD HEIGHT MTRS
8	20250	B	1	13.1	24.7	0.4	0	52
8	20250	E	2	38.2	46.2	1.3	0	44
8	20250	H	1	12.9	22.1	0.5	0	49
8	20250	J	1	12.3	20.7	0.5	0	48
8	20250	K	0	-0.4	6.4	0.0	0	54
8	20250	M	0	0.0	3.3	0.0	0	32
8	20250	N	0	-0.4	-3.8	0.0	0	48
8	20250	O	0	1.8	26.5	0.0	0	40
8	20250	P	0	1.0	14.3	0.0	0	49
8	20250	Q	0	0.4	11.9	0.0	0	57
8	20260	A	0	4.0	15.7	0.0	0	47
8	20260	B	0	4.5	15.3	0.1	0	42
8	20260	C	0	5.3	20.8	0.1	0	55
8	20260	D	0	0.7	3.2	0.0	2	47
8	20260	E	0	-1.3	17.9	0.0	0	40
8	20260	F	0	-2.3	18.8	0.0	0	34
8	20260	G	1	24.0	37.2	0.8	0	32
8	20260	H	1	30.5	66.2	0.5	0	32
8	20260	J	1	28.8	45.0	0.8	0	40
8	20270	A	1	45.0	133.2	0.4	0	32
8	20270	B	1	28.7	84.9	0.3	0	35
8	20270	C	2	25.9	27.1	1.4	0	45
8	20270	D	0	7.8	24.5	0.1	0	42
8	20270	E	1	4.3	8.4	0.2	0	45
8	20270	F	0	2.9	-3.5	0.0	0	43
8	20270	G	0	4.4	15.0	0.1	0	39
8	20270	H	0	4.6	15.1	0.1	0	43
8	20270	J	1	6.6	6.8	0.8	4	51
8	20270	K	1	6.0	10.5	0.3	0	48
8	20280	A	0	2.0	6.8	0.0	0	55
8	20280	B	0	-0.7	7.9	0.0	0	45
8	20280	C	0	-0.5	7.9	0.0	0	30
8	20280	D	0	1.3	10.3	0.0	0	63
8	20280	E	0	1.4	8.9	0.0	0	43
8	20280	F	0	6.8	30.4	0.1	0	35
8	20280	G	2	20.9	25.6	1.0	0	48
8	20280	H	1	18.2	22.7	0.9	0	47
8	20290	A	1	57.5	259.5	0.3	0	19
8	20290	B	0	3.2	18.3	0.0	0	43
8	20290	C	0	-1.8	6.7	0.0	0	45
8	20290	D	0	2.0	10.1	0.0	0	61

Estimated depth may be unreliable because the stronger part of the conductor may be deeper or to one side of the flight line, or because of a shallow dip or overburden effects.

McConnell River Area

FLIGHT	LINE	ANOMALY	CATEGORY	AMPLITUDE (PPM) INPHASE	QUAD.	CONDUCTOR CTP MHOS	DEPTH MTRS	BIRD HEIGHT MTRS
8	20290	E	0	1.9	13.8	0.0	0	56
8	20290	F	1	3.7	4.7	0.4	17	43
8	20290	G	0	8.0	31.2	0.1	0	29
8	20290	H	1	6.0	13.0	0.2	0	41
9	20300	C	0	1.4	8.7	0.0	0	50
9	20300	D	0	-2.6	8.2	0.0	0	58
9	20300	E	0	-0.9	7.5	0.0	0	44
9	20300	F	0	1.5	9.4	0.0	0	47
9	20300	G	0	-3.0	7.2	0.0	0	37
9	20300	H	0	0.1	15.0	0.0	0	47
9	20310	B	0	3.7	11.4	0.1	0	41
9	20310	C	0	5.1	17.1	0.1	0	37
9	20310	D	2	5.2	3.9	1.2	23	44
9	20320	C	0	1.7	0.0	31.0	56	69
9	20320	D	1	5.2	7.3	0.4	7	44
9	20320	E	1	3.5	8.0	0.2	2	42
9	20320	F	0	0.7	7.5	0.0	0	55
9	20320	G	0	0.7	4.7	0.0	6	32
9	20320	H	0	1.2	22.5	0.0	0	39
9	20330	B	0	0.0	6.6	0.0	0	38
9	20330	C	0	2.9	10.8	0.0	0	56
9	20330	D	0	2.2	9.9	0.0	0	41
9	20330	E	0	3.0	7.3	0.1	0	55
9	20330	F	1	4.7	9.4	0.2	0	48
9	20340	C	0	-3.8	7.9	0.0	0	48
9	20340	D	0	0.0	13.8	0.0	0	51
9	20340	E	0	-1.0	10.4	0.0	0	48
9	20340	F	0	2.7	9.6	0.0	0	47
9	20340	G	0	0.2	11.4	0.0	0	43
9	20350	C	0	-0.7	6.2	0.0	0	41
9	20350	D	0	-2.7	8.0	0.0	0	54
9	20350	E	0	0.2	9.7	0.0	0	57
9	20350	F	0	3.3	13.6	0.0	0	50
9	20360	A	0	4.3	19.6	0.0	0	43
9	20360	B	0	2.1	13.5	0.0	0	48
9	20360	C	0	3.2	7.3	0.1	0	59
9	20370	A	0	1.4	5.3	0.0	12	32

Estimated depth may be unreliable because the stronger part of the conductor may be deeper or to one side of the flight line, or because of a shallow dip or overburden effects.

McConnell River Area

FLIGHT	LINE	ANOMALY	CATEGORY	AMPLITUDE (PPM) INPHASE	QUAD.	CONDUCTOR CTP MHOS	DEPTH MTRS	BIRD HEIGHT MTRS
9	20370	B	0	1.4	13.3	0.0	0	55
9	20370	C	0	8.0	25.2	0.1	0	42
9	20370	D	0	2.6	7.2	0.1	14	29
9	20380	A	0	0.3	8.0	0.0	0	38
9	20380	B	0	2.6	14.6	0.0	0	32
9	20380	C	0	2.7	9.3	0.0	0	44
9	20390	A	0	0.0	14.3	0.0	0	49
9	20390	B	0	6.0	16.9	0.1	0	49
9	20400	A	0	2.0	9.7	0.0	0	39
9	20400	B	0	3.6	10.1	0.1	0	42
9	20420	A	0	2.4	26.6	0.0	0	31
9	20420	B	0	2.8	24.2	0.0	0	34
9	20420	C	0	2.8	1.7	1.2	45	44
9	20430	A	0	-8.6	15.4	0.0	0	30
9	20440	A	0	10.3	70.7	0.0	0	29
9	20440	B	0	5.9	22.7	0.1	0	36
9	20440	C	1	5.7	7.9	0.5	9	40
9	20440	D	0	2.2	9.5	0.0	0	44
9	20440	E	1	2.2	4.0	0.2	20	39

Estimated depth may be unreliable because the stronger part of the conductor may be deeper or to one side of the flight line, or because of a shallow dip or overburden effects.

APPENDIX III

CERTIFICATE OF QUALIFICATIONS

I, KEVIN J. KILLIN, certify that: -

1. I hold a B. Sc. (Hons.) in Geological Geophysics from the University of Western Ontario. I also attended University of Toronto as a full-time student during which time I obtained credits in geology.

2. I reside at 255 Grey Squirrel Place in the city of Waterloo, Ontario.

3. I have been engaged in a professional role in the oil and minerals industry in Canada for the past four years.

4. I have been a member of the Prospectors & Developers Association since 1984.

5. The accompanying report was prepared from information supplied by Granges Inc. and from a review of the proprietary airborne geophysical survey flown by Aerodat Limited for Granges Inc. I have not personally visited the property.

6. I have no interest, direct or indirect, in the property described nor do I hold securities in Granges Inc.

Signed,

Kevin J. Killin
Geophysicist

Mississauga, Ontario
September 13, 1990

APPENDIX IV

PERSONNEL

FIELD

Flown	August 15 - August 23, 1990
Pilot	Del Rokosh
Operator	Mark Barry

OFFICE

Processing	Kevin Killin George McDonald
Report	K. Killin
Interpretation	Kevin Killin, Geophysicist

N

5500
4000
3500
4500
4800
5800
4000
4500
636000.
6822000
638000.
6823000
631000.
6818000
637000.
6817000
1917
1864
1444
1400
1012
1300
1400
1100
1100
1200
McCONNELL
WHITE
CREEK

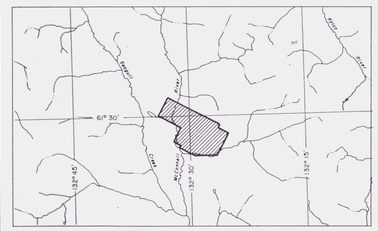

GRANGES INC.

BASE MAP

092879

McCONNELL RIVER

YUKON TERRITORY

SCALE 1:10,000

0 330 660 1320 2640 Feet

0 100 200 500 1000 Metres

AERODAT LIMITED

DATE: AUGUST 1990

NTS No: 105 F/9 F/10

MAP No: 1 J9063 - 1

MAP105F 189,10 Doc# 093879 (834)

N

Flight Path

Flight path recovery from VHS video tape.

Average terrain clearance 60m
Average line spacing 100m

EM Anomalies

Conductivity Thickness (mhos)

- 0 - 1
- 1 - 2
- 2 - 4
- 4 - 8
- 8 - 15
- 15 - 30
- + 30

EM Anomaly A, 4600 Hz (Horizontal coplanar) 100m. Conductivity thickness (1-2 mhos (see code).

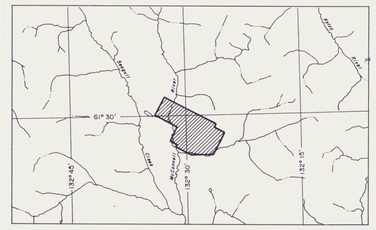

GRANGES INC.

FLIGHT PATH 092879

McCONNELL RIVER

YUKON TERRITORY

SCALE 1:10,000

0 330 660 1320 2640 Feet

0 100 200 500 1000 Metres

AERODAT LIMITED

DATE: AUGUST 1990

NTS No: 105 F/9 F/10

MAP No: 2 J9063 - 1

MAP#105F7,8,9,10 Doc#092879 (235)

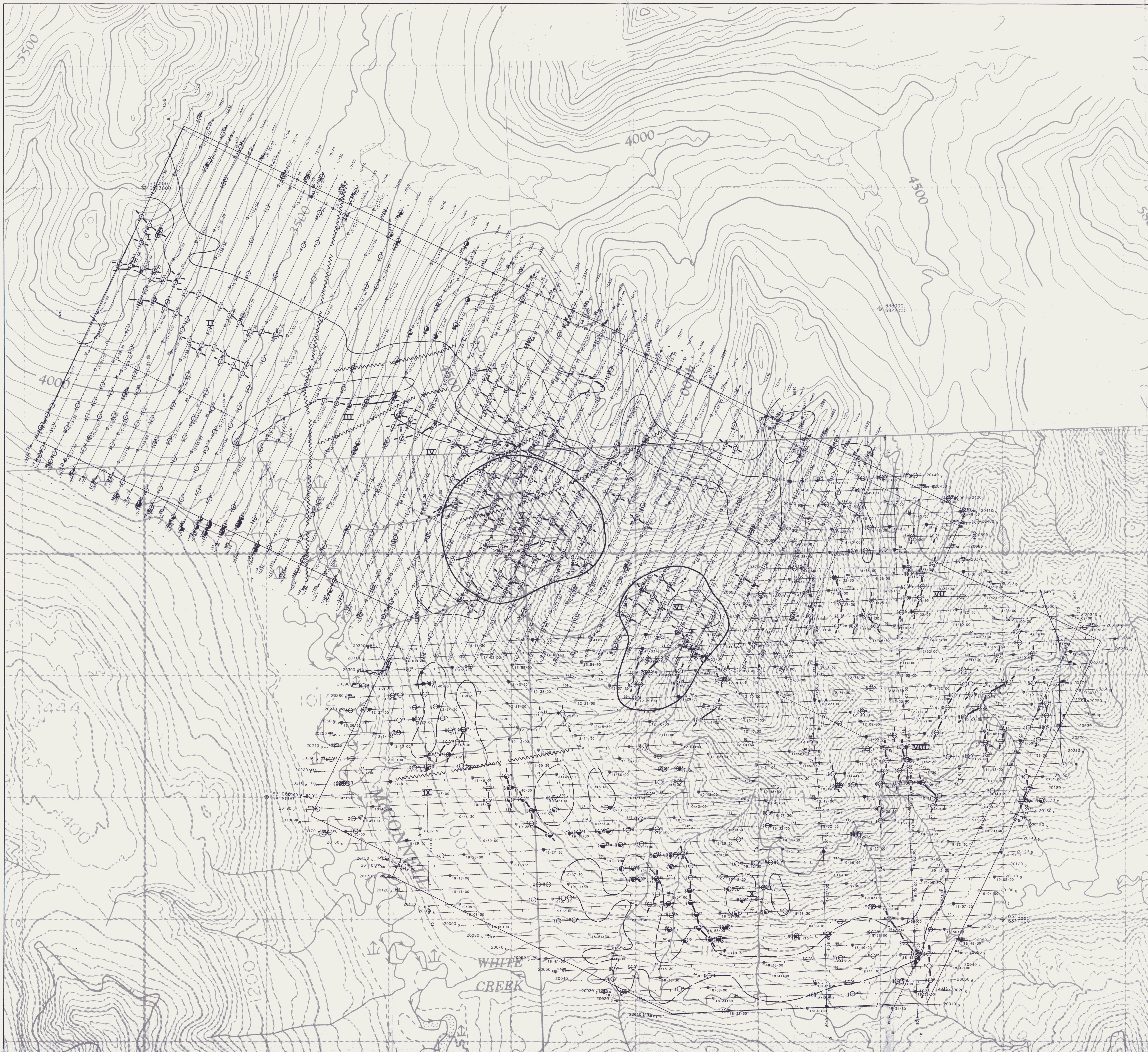

Flight Path

Flight path recovery from VHS video tape.

Average terrain clearance 60m
Average line spacing 100m

EM Anomalies

Conductivity Thickness (mhos)

- 0 - 1
- 1 - 2
- 2 - 4
- 4 - 8
- 8 - 15
- 15 - 30
- > 30

EM Anomaly A, 4600 Hz inphase amplitude 7 ppm. Conductivity thickness 1-2 mhos (see code).

INTERPRETATION LEGEND

- Conductor Axis
- Fault
- Geophysical Contact
- Magnetic Anomaly
- Conductive Zone

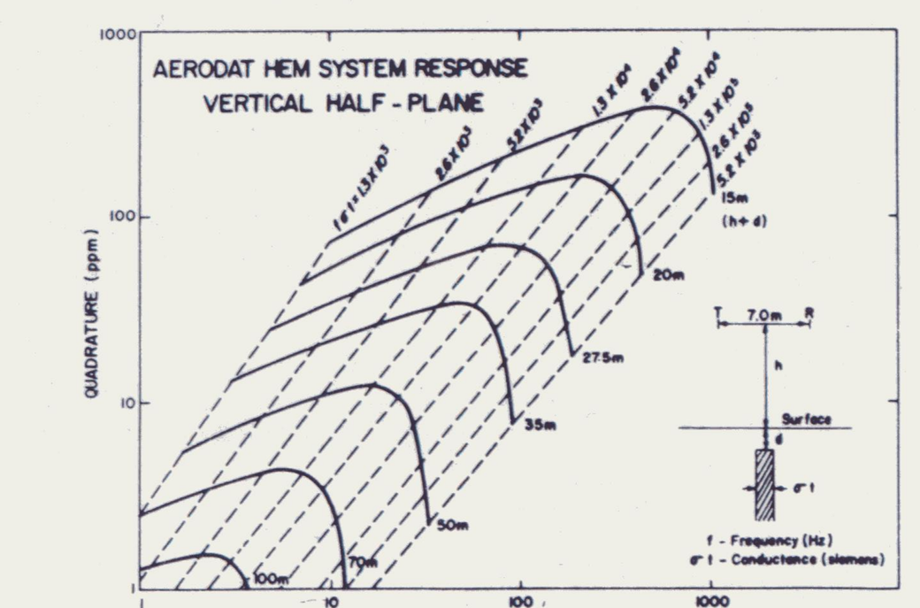

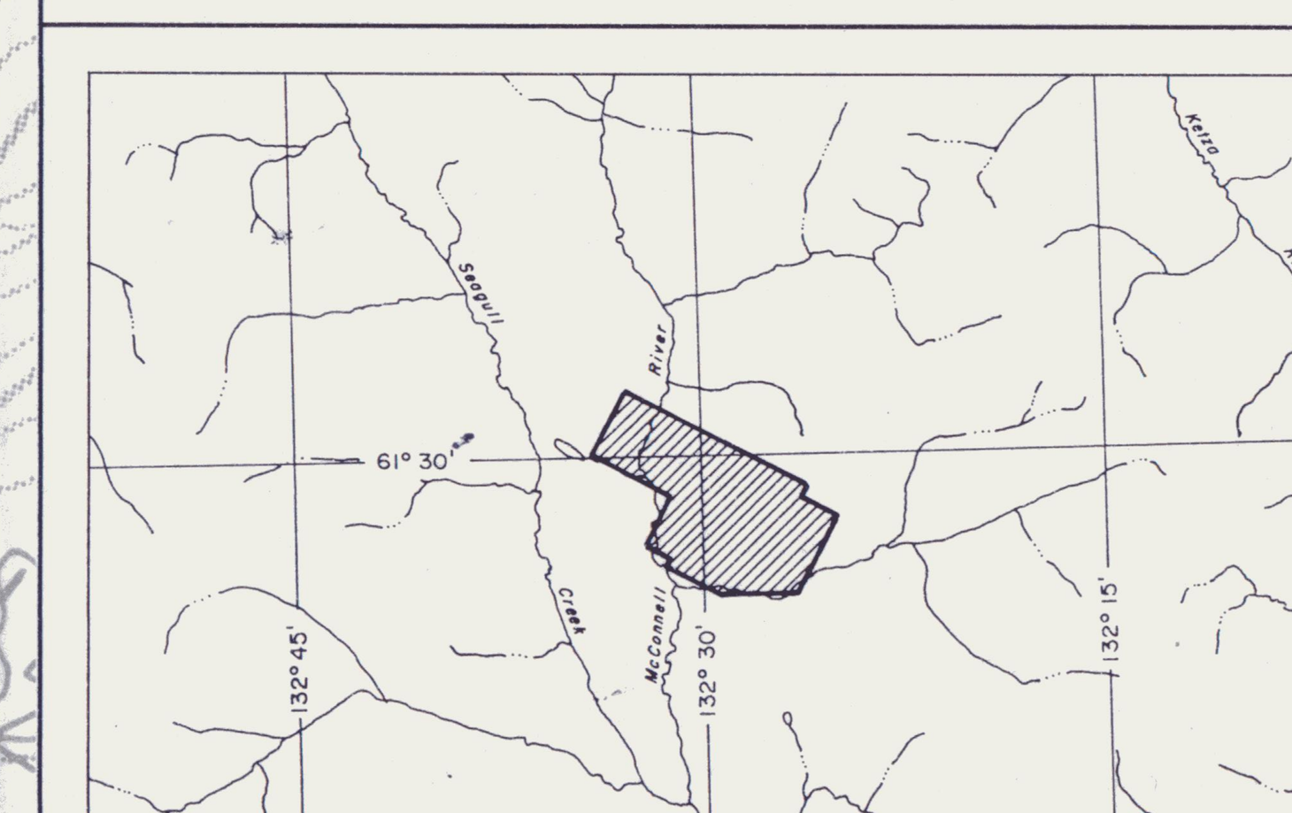

GRANGES INC. 092879

INTERPRETATION

McCONNELL RIVER

YUKON TERRITORY

SCALE 1:10,000

0 330 660 1320 2640 Feet

0 100 200 500 1000 Metres

AERODAT LIMITED

DATE:	AUGUST 1990
NTS No:	105 F/9 F/10
MAP No:	3 J9063 - 1

MAP# 105F 7,8,9,10 Doc# 092879 (236)

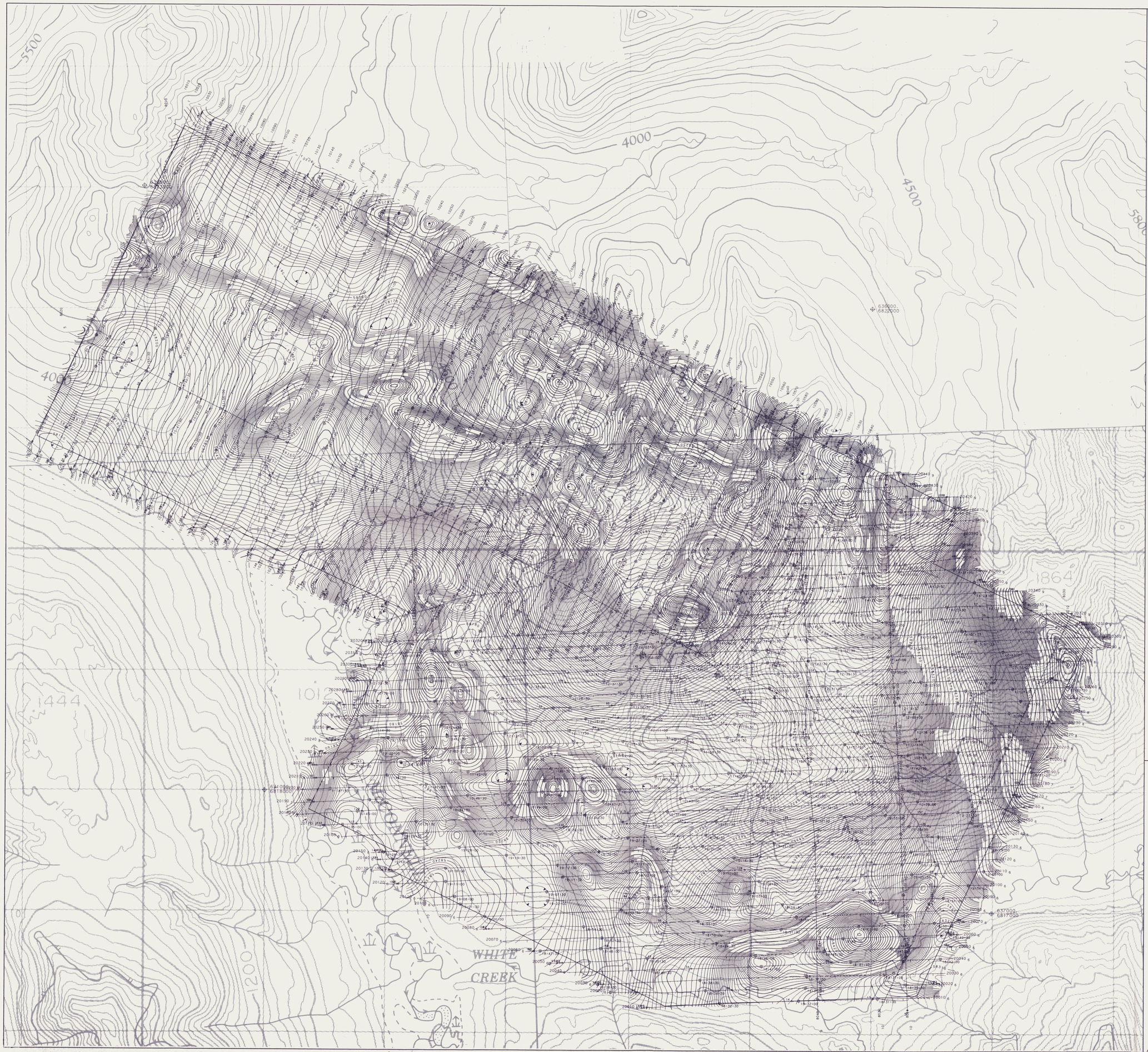

N

Flight Path

Flight path recovery from VHS video tape.

Average terrain clearance 60m
Average line spacing 100m

Magnetics

Total Field Magnetic Intensity Contours in nT.

Cesium high sensitivity magnetometer.

Sensor elevation 45m

Map contours are multiples of those listed below

- 2 nT
- 10 nT
- 50 nT
- 250 nT
- 1000 nT

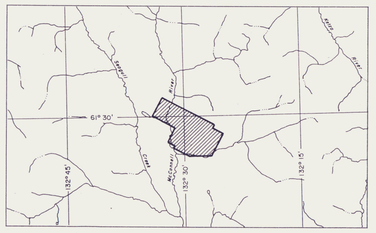

GRANGES INC. 092879

TOTAL FIELD MAGNETIC CONTOURS

McCONNELL RIVER

YUKON TERRITORY

SCALE 1:10,000

0 330 660 1320 2640 Feet

0 100 200 500 1000 Metres

AERODAT LIMITED

DATE: AUGUST 1990

NTS No: 105 F/9 F/10

MAP No: 4 J9063 - 1

Map# 105 F 7,8,9,10 Doc #092879 (237)

N

Flight Path

Flight path recovery from VHS video tape.

Average terrain clearance 60m
Average line spacing 100m

Vertical Gradient

Vertical Magnetic Gradient calculated from the total field megnetic intensity in nT/m.

Cesium high sensitivity magnetometer.

Sensor elevation 45m

Map contours are multiples of those listed below

- 0.100 nT
- 0.500 nT
- 2.500 nT
- 10.00 nT
- 100.00 nT

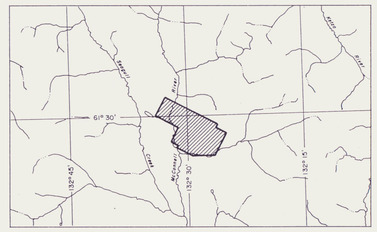

GRANGES INC. 092879

CALCULATED VERTICAL MAGNETIC GRADIENT

McCONNELL RIVER

YUKON TERRITORY

SCALE 1:10,000

0 330 660 1320 2640 Feet

0 100 200 500 1000 Metres

AERODAT LIMITED

DATE: AUGUST 1990

NTS No: 105 F/9 F/10

MAP No: 5 J9063 - 1

MAP# 105F 7,8,9,10 Doc# 092879 (238)

Flight Path

Flight path recovery from VHS video tape.

Average terrain clearance 60m
Average line spacing 100m

VLF-EM

VLF-EM Total Field Intensity in percent.

Station: NPM
Lualualei, Hawaii
23.4 kHz

Sensor elevation 45m

Map contours are multiples of those listed below

1 %
5 %
25 %
100 %

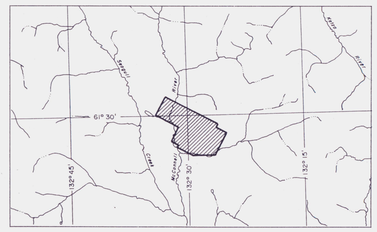

GRANGES INC.

VLF-EM TOTAL FIELD CONTOURS (LINE CHANNEL)

092879

McCONNELL RIVER

YUKON TERRITORY

SCALE 1:10,000

0 330 665 1320 2640 Feet
0 100 200 500 1000 Metres

AERODAT LIMITED

DATE: AUGUST 1990
NTS No: 105 F/9 F/10
MAP No: 6 J9063 - 1

Map#105F 7,8,9,10 Doc#092879 (239)

N

Flight Path

Flight path recovery from VHS video tape.

Average terrain clearance 60m
Average line spacing 100m

Apparent Resistivity

Calculated from 4600 Hz coaxial EM response assuming a 200 m conductive layer.

Contouring in ohm-m at logarithmic intervals.

Sensor elevation 30m

Map contours are multiples of those listed below.

- 0.1 log(ohm-m)
- 0.5 log(ohm-m)
- 2.5 log(ohm-m)
- 5.00 log(ohm-m)

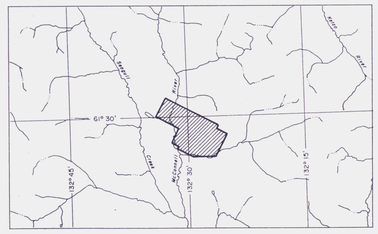

GRANGES INC. 092879

APPARENT RESISTIVITY CONTOURS (4600 Hz)

McCONNELL RIVER

YUKON TERRITORY

SCALE 1:10,000

0 330 660 1320 2640 Feet
0 100 200 500 1000 Metres

AERODAT LIMITED

DATE: AUGUST 1990
NTS No: 105 F/9 F/10
MAP No: 7 J9063 - 1

MAPH 105 F 7,8,9,10 Doc # 092879 (240)

APPENDIX C

AERODAT INVOICE 21-9063-0284

AERODAT LIMITED

3883 NASHUA DRIVE • MISSISSAUGA • ONTARIO • CANADA • L4V 1R3
Telephone: (416) 671-2446 Telex: 06-968872 Fax: (416) 671-8160

Invoice No: 21-9063-0284
Date: September 5, 1990

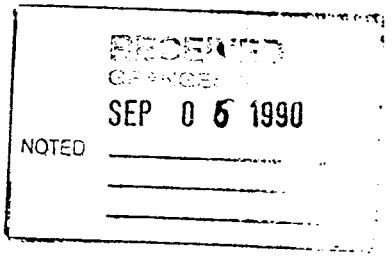

GRANGES INC.
885 West Georgia Street
23rd Floor
Vancouver, B.C.
V6C 3E8

Attention: Mr. Art O'Donnell

In Account With:

Aerodat Limited
3883 Nashua Drive
Mississauga, Ontario
L4V 1R3

Re: Airborne Geophysical Survey - McConnell River Area, Yukon Territory

Mobilization/demobilization	$ 6,000.00
Survey charges 370 km @120.00/line km	$44,400.00
	$50,400.00
Less Invoice 21-9063-0271	$11,500.00
Less Invoice 21-9063-0272	$23,000.00
	$34,500.00
AMOUNT DUE	**$15,900.00**

AS